A ROLE FOR N-GLYCOSYLATION IN DIFFERENTIAL GROWTH CONTROL AND *DROSOPHILA* DEVELOPMENT: PHENOTYPIC ANALYSIS OF ALG10

by

Evan P. Lebois

Approved: Erica M. Selva

Erica M. Selva, PhD.
Professor in charge of thesis on behalf of the Advisory Committee

Approved: David W. Smith

David W. Smith, PhD.
Committee member from the Department of Biological Sciences

Approved: Marlene G. Emara

Marlene G. Emara, PhD.
Committee member from the Board of Senior Thesis Readers

Approved: Rhonda Hyde

Rhonda Hyde, PhD.
Chair of the University Committee on Student and Faculty Honors

TABLE OF CONTENTS

Chapter

LIST OF TABLES

LIST OF FIGURES

ABSTRACT

This study begins to phenotypically characterize mutations in *alg10*, a gene that encodes the enzyme that adds the terminal glucose residue to the growing dolichol-linked oligosaccharide during N-glycosylation prior to its *en masse* transfer to a nascent polypeptide. Genetic and molecular approaches were developed to characterize the *alg10* loss of function phenotype during *Drosophila* development. While pleotrophic phenotypes were observed in *alg10* mutant embryos, clonal analysis of the *alg10* mutation in the developing wing yielded a smaller and rounder adult wing phenotype as compared to wild type. This suggests a potential link between glycosylation and pathways governing growth control. Both the Insulin receptor (InR) signaling pathway and the Epidermal growth factor pathway acting through c-myc are known to control growth in *Drosophila*, roles that are conserved in mammals. To begin to address whether mutations in *alg10* disrupt InR signaling, I examined the genetic interaction between *alg10* and an activated form of InR that produced large disordered eyes. By removing half the Alg10 activity from this background, an enhanced phenotype was observed with an irregular eye surface, fused ommatidia, and patches of necrotic tissue. This indicates a genetic interaction between *alg10* and the dInR pathway and suggests *alg10* influences InR mediated growth control.

Chapter 1

INTRODUCTION

1.1 *Drosophila* Development: an Overview

Using *Drosophila melanogaster* as a model genetic organism is becoming increasingly popular in the modern world of genetics. A rather powerful – and desirable – feature of this organism is that it affords the experimenter with a system bearing a striking level of homology to higher eukaryotic systems all while providing a quick life cycle. In addition to this, a variety of genetic experimental approaches can be carried out using *Drosophila* which are not yet feasible in other organisms. Shown below in Figure 1 is a generalized schematic of the *Drosophila* life cycle where one should note that complete embryo formation is evident merely 24 hours post-fertilization and metamorphosis is occurring just 9 days post-fertilization [1].

In general, genetic manipulation of developing *Drosophila* occurs at points prior to pupa formation. Once pupation occurs, the vitellin membrane (outer casing) hardens to form a protective shell which makes any kind of immunohistochemical staining and visualization impossible [1]. For the purposes of my research, embryonic development as well as the 1st and 3rd instar larvae stages will be the focus.

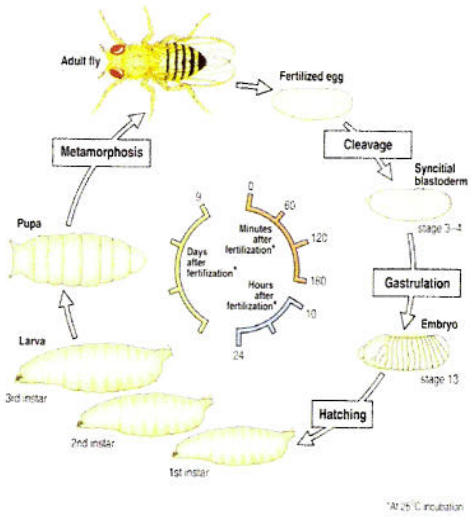

Figure 1: Schematic of *Drosophila* Lifecycle. 0 on the time scale is represented as the point of fertilization. At 180 min post-fertilization Gastrulation occurs, with embryo formation subsequently following at 10 hr. 1st instar larvae are seen at 24 hr, 3rd instar larvae at approximately 3 days. At 9 days pupae are undergoing metamorphosis into adult flies [2].

The primary thrust of embryonic development is to establish a body plan executed by the action of embryo-wide morphogenetic gradients that determine proper development in the adult (Fig. 2A). Proper completion of the embryonic development program can be visualized by the regular series of denticle bands found in the embryonic cuticle upon completion of embryogenesis (Fig. 2B). These denticle bands are the physical manifestation of cellular signaling events in the form of morphogen gradients that sweep along the entire length of the embryo to coordinate all developmental processes [1].

It should be noted here that in wild type (WT) embryos, there is a very precise pattern of denticle banding. Thus, any deviations from this crisp patterning can be interpreted as defects in developmental signaling of denticle

band formation. The developmental consequence of such signaling events is that gastrulation is driven to yield morphologically distinct segments at the end of embryogenesis (Fig. 2A). As one can see from Fig. 2A, these distinct segments correspond to particular regions of the adult fly that is the end product of development [1].

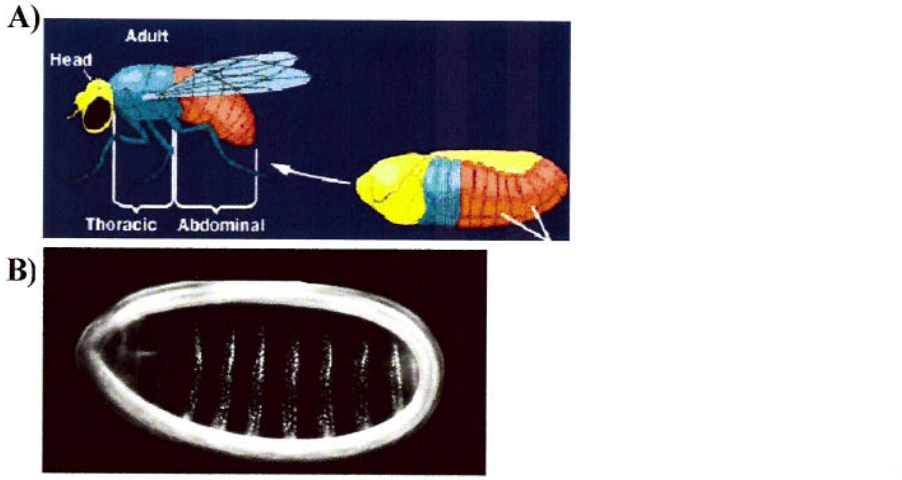

Figure 2: Specification of cell fate in embryogenesis. A) WT embryo showing denticle band formation **B)** embryo post-gastrulation showing morphologically distinct segments [3].

However, between the morphologically segmented embryo and the adult fly lie the stages of larval development noted earlier (Fig. 1). In addition to the embryonic stage just described, these larval stages allow the application of powerful genetic tools. The formation of 1st instar larvae marks the beginning of terminal differentiation in cell type. This terminal differentiation comes in the form of imaginal disc generation. Imaginal discs appear as very tiny disc-shaped structures along the length of the larvae that are morphologically distinct and give rise to the body parts of the adult fruit fly (Fig. 3) [1,4].

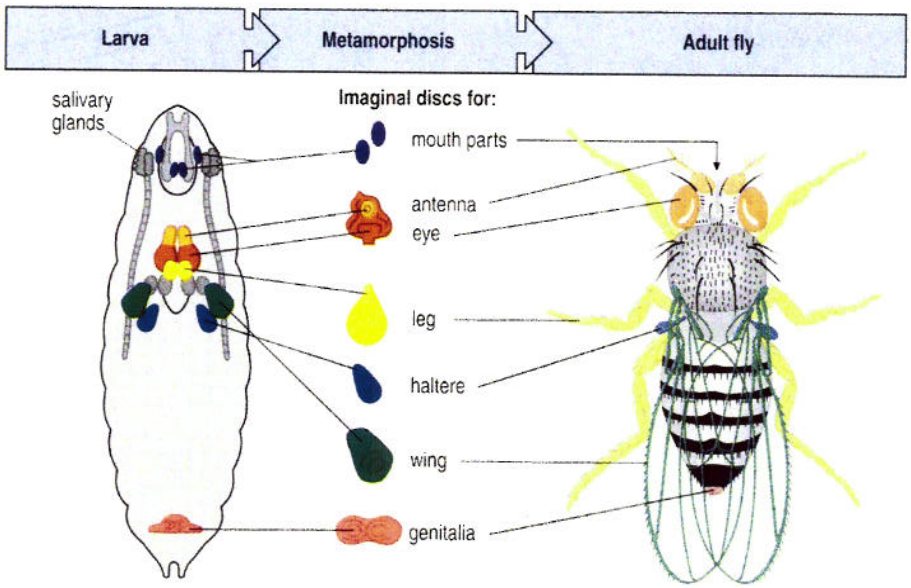

Figure 3: Imaginal disc generation. Lines indicate the origin of the particular disc in the larva and their subsequent fate in the adult. Note the positioning and character of the wing disc [5].

Thus, imaginal discs provide the geneticist with a powerful developmental tool. Developmental processes of higher eukaryotes are reflected beautifully in imaginal discs such as eye formation, nervous system patterning and limb generation. Dissection of any imaginal disc is possible, but perhaps the most common is the wing disc because of its larger size and comparable ease of manipulation (Fig. 3). Since the peak of larval development occurs in the 3rd instar larval stage, this is the stage of choice for wing disc dissection because it allows for maximal growth of the disc. This increased size allows both easier dissection and more detailed visualization. Since the imaginal wing disc is essentially a monolayer of cells it proves to be very amenable to immunohistochemical staining for cellular signaling processes of interest [6,7].

1.2 Maternally Loaded Genes: Early Identification of Loss of Function Phenotypes

During the course of evolution, *Drosophila* have evolved a potential safeguard in an attempt to sustain the maximal number of eggs possible through early development. This safeguard comes in the form of maternal loading of gene transcripts of roughly 30 percent of the *Drosophila* genome into developing eggs. Bearing this in mind, a primary goal of any phenotypic analysis of a lethal mutation is to determine the earliest stages of development at which cellular signaling becomes disrupted in order to halt development.

Thus, if one has a recessive lethal mutation that one is attempting to characterize it is of great importance to know whether or not the mutation of interest lies in a gene that has a maternally loaded transcript. If the mutation of interest is, in fact, in a maternally loaded gene it is immediately apparent that having a multitude of maternally loaded wild type transcripts around could present a profound problem for analysis. The crux of this problem is that even though the embryo may be homozygous for the lethal mutation, the wild type transcripts present will act to sustain the embryo to a later stage of development than would otherwise be possible in their absence. This temporary rescue of the homozygous mutant embryo conceals the true earliest stage of interest at which cellular signaling becomes disrupted and would likely prove both very misleading and very fruitless for analysis if these transcripts are not eliminated [1,8]. Fortunately, genetic methodologies have been developed in the fly to overcome this problem.

1.3 Asparagine(N)-Linked Glycosylation and Significance

Aside from changes in their primary amino acid sequences, proteins can be modified in other manners so as to alter their function, location or stability. One of these critically important ways that proteins are altered is through the implementation of posttranslational modifications, i.e. any chemical alterations made to a protein following translation. A few examples of such alterations are: methylation [9], phosphorylation [10], heparin sulfate addition, sulfation [11] and glycosylation [12]. Glycosylation may be further subdivided into O-linked and N-linked. O-linked glycosylation refers to the attachment of glycans (sugar modifications) onto Ser/Thr side chains. N-glycosylation on the other hand refers to attachment of glycans to an Asn side chain by way of an Asn-X-Ser/Thr consensus sequence where X can be any amino acid except Pro [13,14].

N-linked Glycosylation is a stepwise process that occurs in the ER (Fig. 4). The process begins with a Dolichol anchor on the cytosolic face of the ER that receives two GlcNAc residues from nucleotide-activated sugars and is then mannosylated by Asparagine-linked glycosylase (Alg) enzymes. Following the cytosolic mannosylation, Flippases flip the growing sugar modification into the lumen of the ER where successive action of various Alg enzymes in conjunction with particular nucleotide activated sugars work together to build up the mature sugar modification. Once the sugar modifications are complete, an Oligosaccharyltransferase (OST) enzyme is responsible for their *en masse* transfer to growing poypepetide chains.

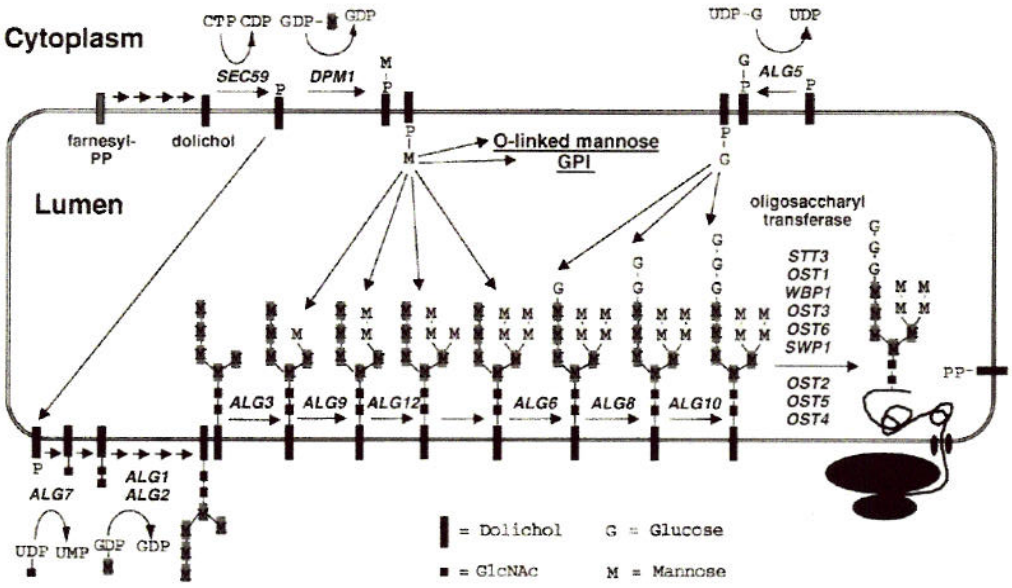

Figure 4: Scheme of N-linked glycosylation. Shown is the lipid-linked oligosaccharide and its *en masse* transfer to a protein at the membrane of the ER. The origin of mannose residues is indicated by shading. Light shading = directly from GDP-Mannose, Dark shading = from dolichylphosphomannose [12].

Polypeptides destined to become glycoproteins bear Asn-X-Ser/Thr glycosylation consensus sequences that are recognized by the OST enzyme. An important thing to note is that the process of glycosylation is cotranslational. Thus, as the protein is being translated, sugar modifications are simultaneously being built up and the OST is monitoring the protein for places to attach sugars. Since proteins begin folding as soon as their nascent amino acid sequence exits the ribosome, it comes as no real surprise that these added glycans are often critically important for glycoproteins to properly fold [13,15,16].

Name	Gene defect	OMIM[b]	Activity	On Fig. 1[c]
CDG-Ia	*PMM2*	212065	Phosphomannomutase (Man-6-P → Man-1-P)	I
CDG-Ib	*PMI*	602579	Phosphomannose isomerase (Fru-6-P → Man-6-P)	2
CDG-Ic	*ALG6*	603147	α1-3 Glucosyltransferase	3
CDG-Id	*ALG3*	601110	α1-3 Mannosyltransferase	4
CDG-Ie	*DPM1*	603503	Dolichyl-phosphate-mannose synthase (GDP-Man → Dol-P-Man)	5
CDG-If	*LEC35*	604041	Unknown	6
CDG-IIa	*MGAT2*	202066	β1-2 *N*-acetylglucosaminyltransferase	7
CDG-IIb	*GLS1*	601336	α1-2 Glucosidase	8
LADII/CDG-IIc	GDP-Fuc transporter	266265	Import of GDP-Fuc into Golgi and export of GMP	9
Ehlers–Danlos syndrome (progeroid form)	*XGPT*	130070	Xylose β1-4 galactosyltransferase	10
Galactosemia I	*GALT*	230400	Gal-1-P uridyltransferase (Gal-1-P + UDP-Glc ⇔ UDP-Gal + Glc-1-P)	11
Galactosemia I	*GALE*	230350	Galactose epimerase (UDP-Gal ⇔ UDP-Glc)	12
Galactosemia II	*GALK*	604313	Galactokinase (Gal → Gal-1-P)	13

[a]Glycogen storage diseases do not represent biosynthetic (anabolic) disorders and are not included in this list.

[b]Accession numbers for the 'Online Mendelian Inheritance in man' (OMIM: www.ncbi.nlm.gov/omim/) database are given.

[c]Refer to Fig. 1 in this article to locate the listed activity in the biosynthesis pathway.

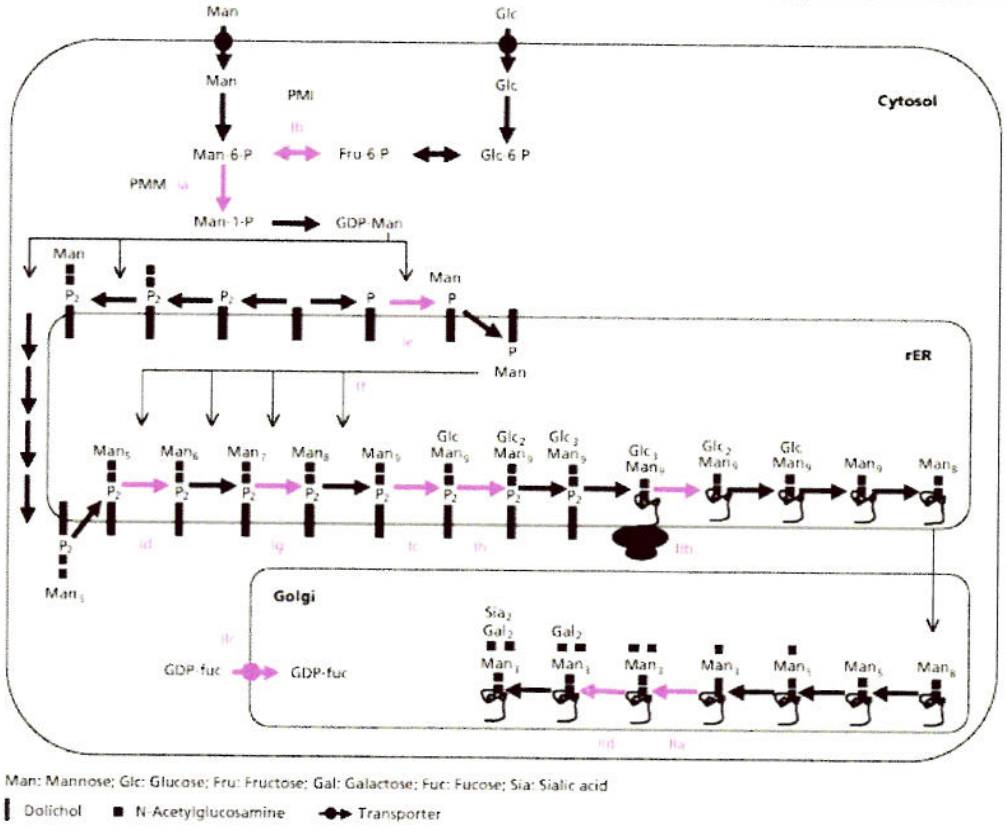

Figure 5: Known Disorders of N-Glycosylation. (top) table showing known disorders of N-glycosylation, gene affected, as well as the process disrupted by the disorder, **(bottom)** pathway from nucleotide activated sugar biosynthesis at top to the pathway of N-linked glycosylation in middle to sugar processing in golgi at bottom. Steps affected by known disorders are highlighted in pink [18].

While the focus of this study is N-linked glycosylation, protein glycosylation as a whole is a fundamentally important posttranslational modification. The field of glycobiology is a relatively new one and gaining interest rapidly. Luis Leloir was awarded the 1970 Nobel Prize in chemistry for first identifying that carbohydrate biosynthesis occurs via nucleotide activated sugars, but it was not until the 1990's with the characterization of congenital disorder of glycosylation-Ia (CDG-Ia) that anyone really had any idea what kind of biological role these sugars were playing with regard to disease (Fig. 5) [17]. Since the identification of this CDG, several others have been identified and glycosylation has been shown to play a chaperone-like role in protein folding, be vital for protein localization and even ligand/receptor and virus/host cell interactions. Since N-glycosylation is such a ubiquitous modification and the single most prevalent modification added to secretory proteins, any defects in N-glycosylation have astounding and far-reaching implications on global biological processes [16,17,18].

1.4 Alg10: What is it and What does it do?

As previously mentioned, when glycans traverse the N-linked glycosylation pathway they are acted on in a stepwise fashion by a variety of different Alg enzymes [19]. Alg10 is one of these Alg enzymes and happens to function as a glucosyltransferase at the very end of the sequence to add the terminal glucose residue onto growing N-glycans. This glucose acts to

complete glycan formation and is the step that immediately precedes their *en masse* transfer by the OST (Fig. 6) [20].

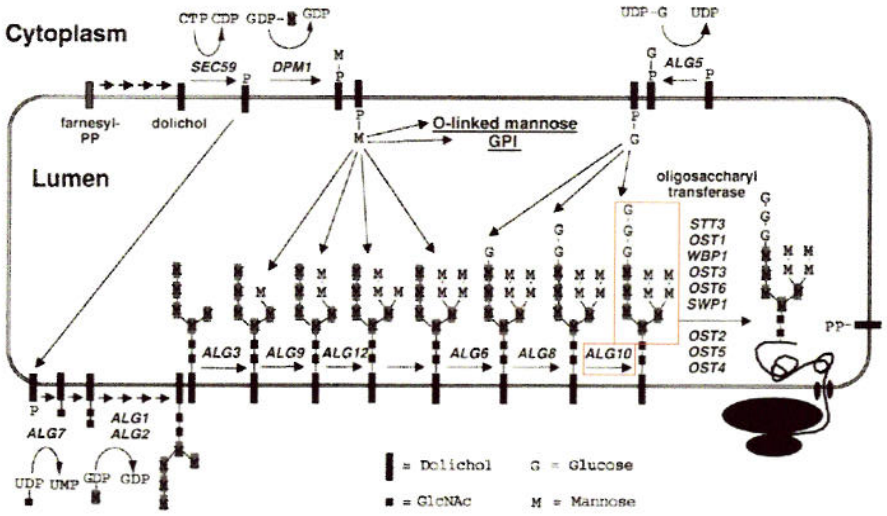

Figure 6: The role of Alg10 in N-linked glycosylation. The step catalyzed by the glucosyltransferase, Alg10, is shown in the red box above. Modified from [13].

1.5 The Oligosaccharyltransferase: A Two-Faced Enzyme in *Drosophila*

The OST enzyme functions at the terminal end of the N-linked glycosylation sequence to catalyze the *en masse* transfer of mature glycans to consensus sequences on nascent polypeptides. This may seem rather straightforward except that, but this is not quite the complete story. In 2003, Kelleher *et. al.* showed that the OST enzyme can actually be comprised of different catalytic STT3 subunits that vary in substrate specificity. In *Drosophila* there are two isoforms of the OST enzyme; one that contains an STT3A catalytic subunit and one that contains an STT3B catalytic subunit.

The significance of these two isoforms is that the STT3A-containing isoform is highly specific, whereas the STT3B-containing isoform is much less-specific [20].

The STT3A isoform will only catalyze the transfer of fully glycosylated substrates. Fully glycosylated here means that the substrates contain all three of the terminal glucose residues put on in the final steps of N-glycosylation (Fig. 7).

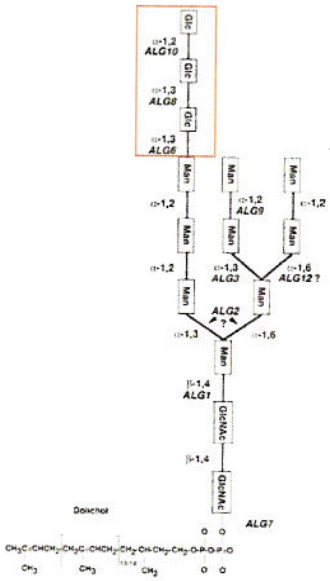

Figure 7: The substrate for N-Glycosylation. The three terminal glucose residues which appear to be critical for OST isoform-specific recognition are shown inside the red box. Modified from [13].

On the other hand, the less-specific STT3B isoform is capable of catalyzing the transfer of hypoglucosylated substrates. Hypoglucosylated here means that the enzyme will transfer substrates that contain any number (0, 1, 2 or 3) of the three terminal glucose residues [20].

Moreover, Kelleher *et al.* postulated that there is some tissue-specific expression of these isoforms whereby expression of the specific isoform is

confined to tissues in high demand of precise glycosylation, i.e. important secretory tissues such as the pancreas and nervous system tissue, whereas the nonspecific isoform is expressed in the remainder of tissues [20].

1.6 Insulin Receptor (InR)/PI3K Signaling

The InR/PI3K pathway is an extremely important growth control pathway in eukaryotic systems. In mammals, insulin and insulin-like growth factors signal through a variety of receptors to mediate proper growth control and metabolic function (Fig. 8A) [21]. Unlike mammals, insects do not have one specific insulin molecule, but rather have a series of Insulin-Like Peptides which are given the name DILPs in *Drosophila*. DILPs1-7 are known to exist and act through a single Insulin-like receptor (dInR) to coordinate proper growth control and proliferation (Fig. 8B) [22,23]. In both systems, such a variety of ligands exists in order to provide a global scheme of cellular growth control and proliferation where the receptor ligands exert their growth control effects in a tissue-specific manner.

This tissue specificity is more finely tuned in mammalian systems where differentiation in signaling molecules occurs in the receptors used and downstream of the InR itself. Simply put, instead of several ligands signaling through one receptor in a tissue-specific manner, mammalian systems instead have one insulin molecule that signals through one receptor. However, the activity of this single InR is complemented by other Insulin-like growth factor receptors (IGFR) with their IGF ligands to further accomplish tissue-

specificity [24,25]. The specialization that occurs downstream of the InR occurs in the form of the Insulin Receptor Substrate (IRS). There are four members of the IRS family known to exist (IRS1-4),

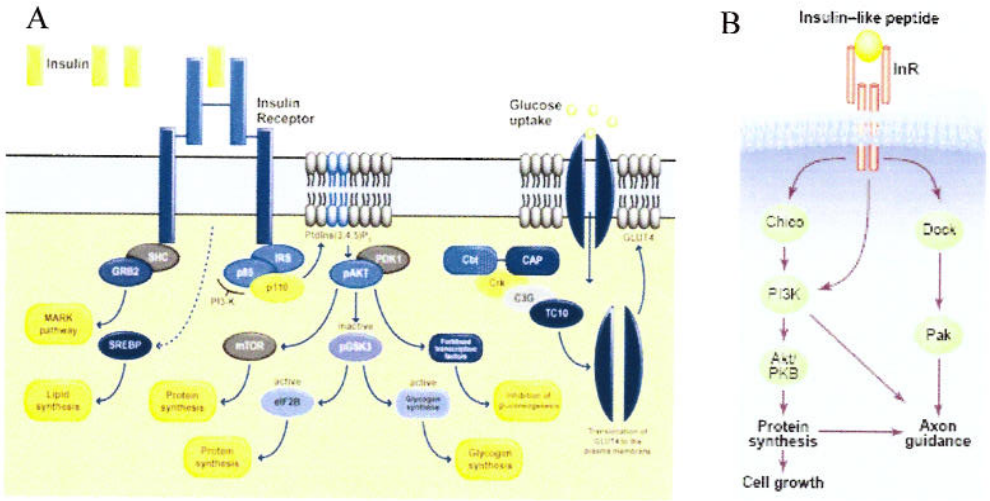

Figure 8: The InR/PI3K pathway. A) The mammalian InR/PI3K pathway. Insulin binding causes IRS adaptor recruitment which allows PI3K to bind and become activated [21]. **B)** Schematic showing InR/PI3K signaling in *Drosophila*. Note that the adaptor protein Chico links PI3K to the receptor here [23].

which function in internalization of insulin and IGF signaling by linking SH2 domain-containing proteins to their respective receptors. Insofar as the scope of this work is concerned, emphasis will be placed upon the linking of the SH2 domain-containing PI3K to the InR and the downstream effects of PI3K in this pathway.

Unlike mammals, insects achieve tissue-specific growth control by specializing their signaling upstream of the InR. As previously mentioned a series of seven DILPs exist which function through the same InR. Thus, while insects have these IGF equivalents, they rely upon a very tissue-specific and temporal expression of them in order to mediate growth control (Table 1)

[26]. In addition to signaling through a single InR, insects do not exhibit any IRS-like specialization downstream of it. While there are four IRS proteins in mammals, there is only one homolog in insect systems named Chico (Fig. 8B). Chico thus functions as an adaptor for linking Dp110 (PI3K) to the InR. A striking difference between mammalian and *Drosophila* InRs is that the *Drosophila* InR possesses a C-terminal cytoplasmic extension of 485 amino acids that allows it to activate Dp110 independent of Chico function. While the *in vivo* consequence of this is not yet understood, it remains a great point of interest and is likely to further add to the ability to further distribute tissue growth control assignments [27,28,29].

Table 1: Summary of *dilp* expression in embryos and larvae [22].

Gene	Embryo	Larva
dilp1	no signal	N.D.
dilp2	high signal in midgut, low signal in mesoderm stage 12–16	ubiquitous low signal in imaginal discs, high signal in seven cells of each brain hemisphere and in salivary glands
dilp3	no signal	high signal in seven cells of each brain hemisphere
dilp4	high signal in mesoderm stage 2–6, anterior midgut rudiment	high expression in midgut
dilp5	no signal	high signal in seven cells of each brain hemisphere, moderate signal in gut
dilp6	no signal	low signal in gut
dilp7	ubiquitous (except yolk) low signal, moderate signal in midgut	high signal in ten cells of ventral nerve cord

N.D., not determined

1.7 InR Signaling in *Drosophila* Growth Control and Development

During *Drosophila* development InR signaling is responsible for coordinating organ growth and proper nervous system development. Organs are destined to reach a given terminal size and must do so through regulation of two factors: cell number and cell size. An organ of particular interest in this study is the eye (Fig. 9) [30]. Aside from global development, InR/PI3K signaling plays a particularly critical role in nervous system development and

axonal guidance. InR expression is the equivalent of an electrician within a developing fly, ensuring that the nervous system is properly wired during development. In eye-specific studies, it has been shown that proper InR activity is needed for correct axonal guidance of ommatidial photoreceptors. This ensures a proper link between the retina and the axon target tissue on the brain. Flies mutant for the InR display axonal targeting defects such that the photoreceptor axons veer off course and never make it to their correct targets during eye development [27,29,31,32].

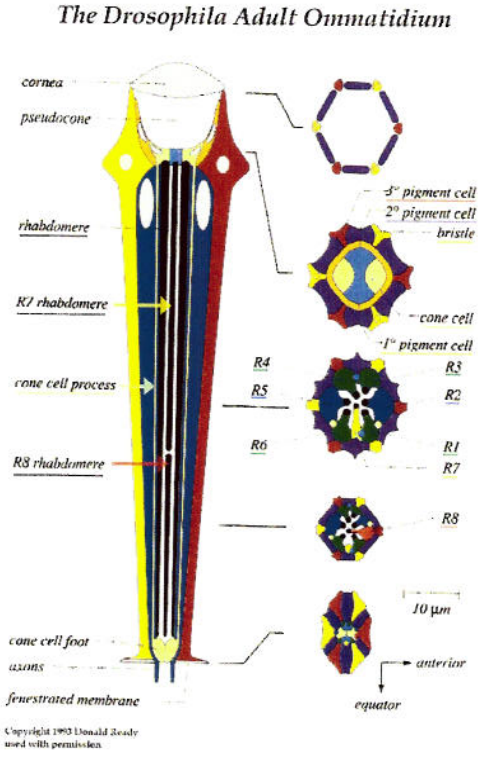

Figure 9: Structure of the adult ommatidium. Shown is photoreceptor cell differentiation as well as proper photoreceptor cell and axon connectivity to the fenestrated membrane [30].

A key component of the InR signaling cascade in *Drosophila* is the forkhead transcription factor FOXO. FOXO has been found to activate the

transcription of both InR and 4EBP, leading to cell cycle arrest in developing flies (Fig. 10). Under high insulin conditions, Akt phosphorylates FOXO to inhibit its transcriptional activity. Conversely, under insulin-deprived conditions, FOXO is activated and transcriptionally activates InR and 4EBP expression which leads to cell cycle arrest. Interestingly it has been shown that by targeting FOXO expression in developing flies, resulting organ size results from a specification of cell number and not cell size [33,34].

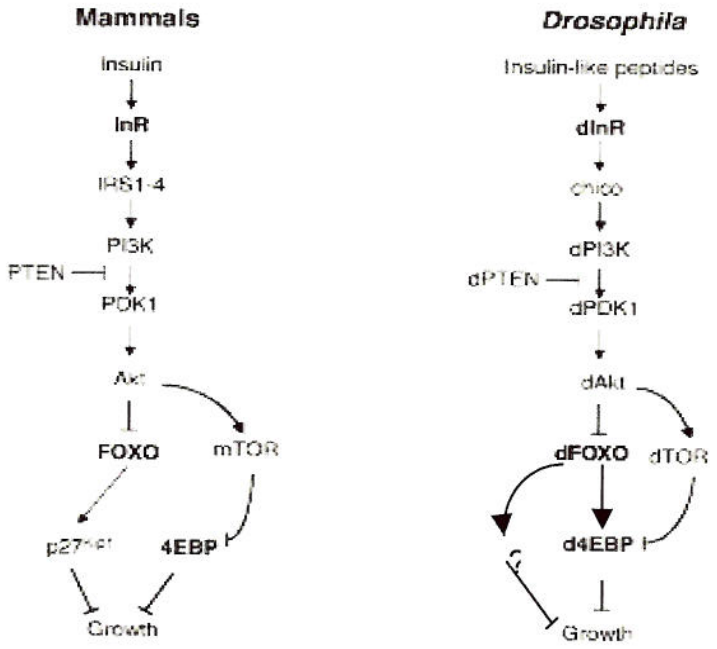

Figure 10: FOXO as a regulator of cell growth. Shown is a schematic detailing the role of FOXO in both mammalian and *Drosophila* systems. Of interest is the manner in which FOXO feeds back on the InR itself to transcriptionally activate it [35].

1.8 Creation and Characterization of *alg10* Mutations

Shown below in Figure 11 is the *alg10* genomic region. As one will note, the red triangle represents the location of the P-element used in this study. By utilizing imprecise P-element mediated excision, a series of five mutations in *alg10* was generated in our laboratory. These mutations were given the names Δalg10-5, Δalg10-7, Δalg10-10, Δalg10-17 and Δalg10-27.

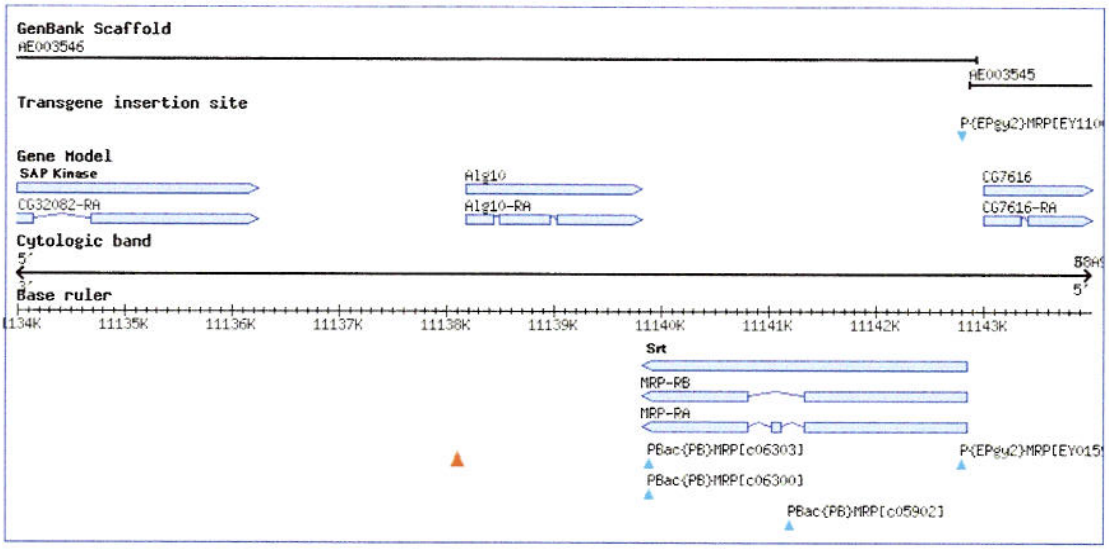

Figure11: The *alg10* genomic region. Shown here is the *alg10* genomic region along with the approximate location of the P-element (red triangle) used in this study. Note its relatively close proximity to the *alg10* gene.

The premise of P-element mediated excision is that during P-element excision, when the P-element of interest excises, flanking DNA is taken along with it. Moreover, often times P-elements will seem to preferentially excise more to one side than another, appearing to have some directionality associated with them. Based upon preliminary sequence characterization, the mutations generated appear to be null mutations, as they significantly cross into the 5' end of *alg10* to abolish proximal promoter and regulatory elements.

1.9 Specific Aims

When starting this project, I had three specific aims in mind that I wanted to accomplish. First, I wanted to show that Alg10 function is important for *Drosophila* development by employing genetic loss of function techniques. As a follow up to the first, my second aim was to find a specific pathway(s) that was/were disrupted by loss of Alg10 function. By examining the phenotypic effects of the *alg10* mutation in different developmental contexts, the hope was that the disruption could be pinned down to specific developmental pathways. Finally, I wished to show how regulated glycosylation might be a critical mechanism in orchestrating proper organismal development through employing immunohistochemical approaches.

By conducting future studies, it is hoped that this work will shed new light on the role glycosylation plays in a more global context during organismal development. In addition to the fundamental role it plays, a better understanding of how it is regulated in order to achieve the enormous task of tissue and stage-specific growth is hoped to be obtained. Possessing this knowledge will likely be central to determining the etiology and eventual treatment of developmental disorders, particularly those pertaining to nervous system development.

Chapter 2

MATERIALS AND METHODS

2.1 Hairpin RNAi Construct Generation

Unlike classical dsRNA that proves competent for post-transcriptional gene silencing in mammalian systems, regular dsRNA injected into *Drosophila* does not prove as efficient at inducing gene-knockdown. Thus, hairpin constructs are utilized which require construction of an inverted repeat transgene. The construct used in this study is the pWIZ (White Intron Zipper) construct, which takes advantage of a 74bp *white* intron that serves as a functional spacer intron between the inverted repeats that are cloned to either side of it (36). The intron is flanked by multiple restriction sites on either side, enabling easy incorporation of DNA sequences. Incorporation of DNAs corresponding to target sequences of interest were cloned in two separate steps. Sequences against Alg10, Porcupine (Porc) and Wingless (Wg) were used. Also, an *alg10* cDNA under the control of a UAS-Gal4 promoter in a pUAST vector was used in making a gain of function rescue construct.

As mentioned, it was necessary to perform cloning for the hairpin constructs in two separate steps. The general logic of cloning follows the progression that the given insert is cloned in and the orientation is subsequently checked. Then the second insert is cloned in and the orientation checked. Checking the orientation is of vital importance, as when the IR

transgene is ultimately translated *in vivo*, there are only two possible orientations of inserts that will give rise to viable hairpins. The inserts must therefore be head-to-head or tail-to-tail.

In order to generate DNA inserts corresponding to desired target sequences, genomic DNA was isolated from w^{1118}/w^{1118} flies and PCR amplified with corresponding synthesis primers to generate fragments for subcloning (Table 2). Isolation was performed by first homogenizing 20 flies in a solution containing 0.1M Tris pH 8.0, 0.1M EDTA and 1% SDS. The homogenates were then incubated for 30 min. at 70°C. 8M KOAc was then added and the tubes mixed gently. The tubes were then placed on ice for 30 min. and pelleted at 14,000 rpm at 4°C for 15 min. Following this, the supernatant was then transferred to a fresh tube, STRATACLEAN resin added and mixed for 3 min. After, the tubes were spun at 14,000 rpm at 4°C for 1 min. and the supernatant again transferred to a fresh tube. Isopropanol was then added at room temperature (RT), mixed and spun at 15,000 rpm for 5 min. at RT. The pellet that formed was then washed with cold 70% ethanol, air dried and resuspended in TE pH 8.0. A 1:100 dilution of each sample was then made with TE pH 8.0 and the A_{260}/A_{280} determined. DNA isolated from *Δalg10* FRT^{2A}*/TM3* flies was then used in conjunction with the mapping primers in order to map the various deletion mutations (Table 2).

Table 2: Primers used for DNA synthesis, sequencing and QPCR.

Primer Name	Sequence (5'→ 3')	Use
spWIZ-1	ACTCTGAATAGGGAATTGGG	Sequence
spWIZ-2	CATAAGTAAGGTTCCTTCAC	Sequence
spWIZ-new3f	CTATTCGCAGTCGGCTGATCTGTGTGAAAT	Sequence
spWIZ-new4r	CAAAGATAAGCGTCAGCCGACTAGACACAC	Sequence
Alg10-250bpF	ACCAAGGGCCCAGACCATATTCTT	Mapping
Alg10-250bpR	AATCCCTGCGGAATGTGGAACT	Mapping
Alg10-500F	GCAAGCACAGATCCTTCACCAGATGCCCAA	Mapping
Alg10-500R	TGTCCGTGCTTCCGCCGCTCTACTTCTTTA	Mapping
Alg10-1KbF	GTTTAAGCCAAGACTTAGGGTTCCACGAGC	Mapping
Alg10-1KbR	GTATAGTGTCTGTTGTCAGCCAGCAGGTAG	Mapping
Alg10-1500bpF	GTATTTCCAGCCGTAAGTAGTGGTCCCAAG	Mapping
Alg10-1500bpR	CCGTGTGTTGAGTCGAAACAGAATGTACGG	Mapping
F-QPCR-aTubulin	CGCTCTCTGAGTCAGACCTC	QPCR
R-QPCR-aTubulin	ACCAGCCTGACCAACATGGA	QPCR
rtb-CG32076-Alg10-F1	CCTGGTGCCGTACATTCTGT	QPCR
rtb-CG32076-Alg10-R1	CCTTTGAGGAGTGCGGTAGT	QPCR
iWg-F	TAATACGACTCACTATAGGTCTAGAACGTCCAAGCGGAGATGCGA	Synthesis
iWg-R	TAATACGACTCACTATAGGTCTAGATTATGCTTGCGTCCCTGACG	Synthesis
iAlg10F	TAATACGACTCACTATAGGTCTAGAGGTTCCATTGTGGTGGGCGA	Synthesis
iAlg10R	TAATACGACTCACTATAGGTCTAGAAGCTCCAGGAGTCGCTGGAA	Synthesis
iporcF	TAATACGACTCACTATAGGTCTAGATTGAACTCCCTGTCCTACTG	Synthesis
iporcR	TAATACGACTCACTATAGGTCTAGAAGGAGTGCTATCCATTCAGC	Synthesis
cDNA-Alg10-F1	CCAGAATGCGGCCGCATGAATGGGTCCTGGAAACTAATCCTGCCC	Synthesis
cDNA-Alg10-F2	CCAAGAATTCTAGACTACCATATGATCCTTTGAGGAGTGCGGT	Synthesis

To accomplish the cloning 0.5μg of the sequence to be incorporated into the vector was first digested with XbaI, a restriction enzyme corresponding to one of the enzymes of the multiple cloning sites in the pWIZ vector. 1.0μL of the pWIZ vector (0.77μg/μL) was then digested with XbaI in order to generate a complementary end, followed by Shrimp Alkaline Phosphatase (SAP) (Promega) treatment according to the manufacturer's protocol to remove the 5' phosphates on the vector to prevent recircularization. Following SAP treatment, 10μL overnight ligations were performed with 1μL of vector, 1μL of the XbaI-digested fragment of interest, 1μL of 10x ligation buffer, 0.5μL of T4 DNA ligase and 6.5μL of water. 1μL of the ligations was then added to 20μL of DH5α highly competent *E. coli* cells (Invitrogen). The cells were then transformed by electroporation using a BioRad micropulser in a 0.1cm cuvette. Immediately after the pulse, 1mL of LB was added and the cells were then incubated for 1hr at 37°C. After inoculation, 10% and the remainder of cells were plated on LB + 75μg/μL Carbenicillin plates and incubated overnight at 37°C. A plasmid prep was then done on individual recombinant clones using QIAGEN's Plasmid Mini kit according to the manufacturer's protocol in order to isolate and purify the plasmids. The orientation of the insert was then checked using a series of diagnostic double digests.

This process was then repeated for the second insert once the orientation of the first was confirmed. The only difference in the second cloning is that the restriction enzyme NotI is used to digest insert and vector. All subsequent steps remain the same, with appropriate enzymes being selected for the double digests to check orientation. Once the orientation of the second insert was confirmed, DNA sequencing was performed using a

series of four primers (spWIZ-1, spWIZ-2, spWIZ-new3f and spWIZ-new4r) corresponding to pWIZ vector sites (spWIZ-1 and new4r) on either side of our insert as well as within (spWIZ-2 and new3f) the white intron located in the middle of the two inserts in order to molecularly confirm our constructs (Table 2). Sequence analysis of obtained DNA sequences was performed using Sequencher v4.0.

Once the constructs were verified via DNA sequencing, QPCR was performed on the pWIZ-*alg10*, pUAST-*alg10cDNA* and tubulin control primers using the appropriate rtb-CG32076-Alg10-F1 and rtb-CG32076-Alg10-R1 primers in order to verify their activity *in vitro* (Table 2). In order to do this, S2R+ cells were transfected with either the pWIZ-*alg10* hairpin RNAi or the cDNA rescue construct and subjected to QPCR using SYBR Green (QuantiTech) fluorophore and QPCR primers. Mock-transfected S2R+ cells were used as a negative control. The pUAST-*alg10*cDNA rescue construct gave expected upregulation of *alg10* transcription several orders of magnitude; however, the *alg10* hairpin construct failed to substantially suppress the production of Alg10 messages *in vitro* (data not shown).

2.2 Zygotic Lethal Stage Determination

In order to address the biological significance of the glucose transferred by Alg10, loss of function studies were conducted in the context of the developing organism. This experiment essentially compares the ability of homozygous mutant flies to survive as compared to wild type flies. An

overall percent lethality is then tabulated in the form of a ratio of embryos that died during development to the total number of embryos one started with to give an indication of how important Alg10 function is for embryonic development.

To set up the experiment, *Δalg10-10FRT2A/+* virgins were crossed to *Δalg10-10FRT2A/+* males in an embryo collection chamber and allowed to lay overnight (no more than 24hr). Thus, ¼ of the resulting embryos from this cross should be homozygous for the *alg10* mutation. Once a sufficient number of embryos were laid from this cross, 100 random embryos were lined up across the middle of a new collection plate (essentially a small Petri dish) and a spot of yeast was added at the outside of the dish on either side of the line of embryos at the furthest possible point away from them.

After the plate was set up, the embryos were allowed to develop at 18°C for 48 hours after which the plate was examined under a dissecting scope for unhatched embryos. The number of unhatched embryos was then expressed in a ratio to the total number of embryos that were laid across the plate to begin with. This experiment was repeated in triplicate.

2.3 Germline Clones and Embryo Collection

Since *alg10* is known to be a maternally loaded gene, in order to identify the earliest loss-of-function embryonic phenotype the necessity to generate germline clones arose. The reasoning behind generating germline clones is that in doing so, the maternal contribution to the embryo is removed.

Therefore, the earliest stages of disruption from loss-of-function experiments in the developing embryo can be observed. In addition to providing a gross phenotype, knowing the earliest stages of disruption of a loss-of-function mutation can be profoundly helpful in pinpointing processes that may be disrupted.

In order to begin the process of germline clone generation, virgin *ywflp/ywflp;Dr/TM3* females were crossed to *ovo[D1]FRT2A/TM3* males. From this cross *ywflp/+;ovo[D1]/FRT2A/TM3* males were isolated and crossed to *Δalg10-10 FRT2A/ovo[D1] FRT2A* virgin females. Approximately 5-6 days after establishing the cross, the third instar larvae were heat shocked for 1 hour at 37°C in order to induce homologous recombination between FRT sites. The larvae were then allowed to develop to adulthood and *Δalg10-10 FRT2A/ovo[D1] FRT2A* virgin females were identified by the absence of the TM3 balancer. Only those virgins that have undergone recombination in their germline stem cells to lose ovo[D1] yield *Δalg10-10 FRT2A/Δalg10-10 FRT2A* stem cells were capable of producing eggs. These females were then crossed to *Δalg10 FRT2A/TM3 Twi-GFP* males yielding embryos that have no maternal *alg10*. However, half will be hetereozygous for *alg10*, whereas the other half will be homozygous. Embryos were then collected from this cross and dechorionated in 50% bleach for 5 minutes to remove the chorion covering the vitellin membrane and embryonic cuticle and washed thoroughly with water. A portion of the embryos were then taken and mounted in Hoyers and heated at 55°C to remove internal tissue and visualized on a Zeiss

Axiophot light microscope in dark field to document any embryonic cuticle phenotype.

The remainder of the embryos were then fixed for immunohistochemical staining. The embryos were added to a 2mL glass vial containing heptane:PEM-FA (5x PEM {80 mM PIPES [piperazine-N,N′-bis(2-ethanesulfonic acid)], pH 6.8, 1 mM EGTA, and 1 mM $MgCl_2$}, 4% Formaldehyde) in a 1:1 ratio and placed on a shaker for 20 minutes in order to fix the embryos. The bottom aqueous layer was then removed with a Pasteur pipette and replaced with an equivalent volume (1mL) of methanol. Following this, the vial was vortexed for 1 minute in order to crack the embryos out of their vitellin membranes. This is necessary to render the embryos accessible for subsequent immunohistochemical staining because the vitellin membrane would otherwise prevent antibody infiltration to the tissues. The vitellin membranes then fell into the bottom heptane layer and were removed with a Pasteur pipette. Finally, the embryos were washed 3x with methanol and stored at -20°C.

Immunohistochemical staining of embryos with BiP and FasII was then carried out as in **2.4**, in a total volume of 500µL. Rabbit anti-Bip was used at a dilution of 1:100 along with mouse anti-1D4 (FasII) at a dilution of 1:10. Secondary antibodies used were anti-rabbit A594 and anti-mouse A647, both of which were used at a dilution of 1:500.

2.4 Antibody Staining in Larval Clones

In order to create larval clones *Δalg10-10 FRT2A/TM6B,Tb* virgin females were crossed to *ywflp/ywflp;m*^{i55}*hsGFP FRT2A/TM6B,Tb* males and allowed to lay for 3 days until first instar larvae developed. After 3 days the cross was transferred to a new vial and the first instar larvae were heat-shocked for 1 hour at 37°C in order to induce homologous recombination between FRT sites. The significance of this is that the homologous recombination produces patches of homozygous mutant tissue for the duration of the heat-shock in the organism. Approximately 3 days later when the majority of the larvae in the vial are at the third instar stage, the larvae are heat-shocked again for 1 hour at 37°C, but this time the heat-shock is to induce GFP expression. The significance of the GFP is that it marks heterozygous tissue. The patches of homozygous mutant tissue that are generated from the first instar heat-shock will be GFP-negative since the GFP does not segregate with the *alg10* mutation during the heat-shock.

Following the heat-shock, the vial was allowed to sit for 1 hour at room temperature. After cooling, a primary dissection was performed with ~20 larvae in 1x PBT. This entails using a dissecting scope and a pair of precision tweezers to tear the larvae in half just posterior of midsection. Once torn in half, the tweezers are used to turn the larvae inside out by pushing the mouth backward through the body cavity and out midsection. This is done in order to expose the imaginal discs of the larvae to solution such that when subsequent antibodies are added they can readily access the tissues.

Antibodies used for immunohistochemical stainings were mouse anti-wingless (Wg), guinea pig anti-senseless (Sen), mouse anti-engrailed (En), rat anti-Ci and mouse anti-patched (Ptc). The Wg and Sen staining was performed in a 500μL total volume containing 50μL 10x PBT, 25μL NHS, 374.5μL water, 50μL mouse anti-Wg (4D4 1:10 dilution, from DSHB) and 0.5μL guinea pig anti-Sen (1:1000 dilution, from H. Bellen). The En and Ci staining was also performed in a total volume of 500μL which contained 50μL 10x PBT, 25μL NHS, 250μL water, 125μL mouse anti-En (1:4 dilution, from DSHB) and 50μL rat anti-Ci (1:10, from Holmgren). Unlike the former two, the Ptc staining was performed in 1mL total volume which contained 100μL 10x PBT, 50μL NHS, 849.7μL water and 0.3μL mouse anti-Ptc (1:3000 dilution, from D. Strutt).

2.5 Adult Wing Clones

The methodology of adult clone generation follows the larval clone generation exactly. However, the only important difference is that except instead of generating GFP-marked clones for dissection and immunohistochemical staining, the first instar heat shock is delivered to generate patches of homozygous mutant tissue and the larve are then allowed to develop into adult flies. This allows one to investigate phenotypic effects in the context of an adult fly.

In order to begin generating adult clones, *ywflp/ywflp;m^{i55}hsGFP FRT2A/TM3* virgin females were crossed to *Δalg10-10 FRT2A/TM3* males for

2-3 days. Once formation of first instar larvae was noted in the vial, the larvae were heat shocked for 1 hour at 37°C. Following the heat shock, the larvae were allowed to develop into adult flies and then *Δalg10-10 FRT2A/ hsGFP FRT2A* progeny were collected and examined under a dissecting scope for phenotypes in order to aid in determining any potential cell signaling pathways that may have been disrupted. Upon noting similar wing phenotypes, wings were then mounted in euparal (ASCO Laboratories) and documented under a Zeiss Axiophot light microscope in bright field.

2.6 Alg10-InR/PI3K Pathway Genetic Interaction Study

In order to determine if a genetic interaction existed between *alg10* and the dInR, a phenotypic study was performed in the eye. Since the dInR is a known glycoprotein, constitutive eye-specific mutants were obtained for use in this study [35]. *GMR-GAL4/GMR-GAL4;UAS-dInR-A1325D/UAS-dInR-A1325D* (Bloomington Stock #8840) virgin females were crossed to w^{1118}/w^{1118} males in order to establish a baseline for the experiment. This cross generated *GMR-GAL4/+;UAS-dInR/+* flies which allowed us to see the phenotype of our mutation in a background with 100% of *alg10* activity. Once we obtained a baseline phenotype, *GMR-GAL4/GMR-GAL4;UAS-dInR-A1325D/UAS-dInR-A1325D* virgin females were then crossed to *Δalg10-10 FRT2A/TM3* males in order to generate *GMR-GAL4/ +;UAS-dInR/ Δalg10-10 FRT2A* progeny. The significance of performing this cross is to knock *alg10* activity down by 50% and observe whether any change in phenotype takes

place as compared to our baseline phenotype with 100% *alg10* activity, indicating a genetic interaction. For comparison to a normal wild type fly eye, Oregon Red (OR) flies were used and compared to each of the above described mutants.

2.7 Sectioning and Histochemical Staining of Eyes

Since a genetic interaction was observed between *alg10* and the dInR/PI3K signaling pathway, eyes were isolated from the above mutants and several OR flies for histological sectioning. Eyes were fixed and embedded in paraffin blocks by the histology department at A.I. DuPont Children's Hospital. Initial sectioning was performed at A.I. DuPont as well, but additional transverse and tangential sections were required. Subsequent sectioning was performed with assistance from the M. Duncan laboratory, where a microtome was used to cut 6μm tangential sections from the paraffin blocks. After being cut, the sections were placed on a microscope slide and allowed to dry on a slide warmer at 25°C overnight. Once dry, the slides were processed by histochemical staining using a hematoxylin and eosin staining protocol developed by M. Duncan. After staining, the slides were allowed to dry at room temperature for 3 hours and then coverslipped using CytoSeal fixative. The sections were then visualized and photographed under a Zeiss Axiophot light microscope at both 20x and 40x in bright field. The initial transverse sections were also photographed at 20x and 40x in addition to the tangential sections.

2.8 Scanning Electron Microscopy (SEM) of Eyes

Since a gross phenotype was observed in the genetic interaction study with the constitutive mutant, the study was repeated as before with the addition of other components of the dInR/PI3K pathway and analyzed by SEM performed on the resulting eyes. SEM is a more precise diagnostic tool than gross phenotypic analysis, so more information can be gained. Other components of the dInR/PI3K pathway examined were Chico, PTEN, *Δalg10-17* (a second mutation in *alg10*), Akt and PI3K. For this study, it is necessary to prepare the eyes in a certain manner in order to ensure that they can be properly visualized by SEM. First, the flies of the correct genotype were flipped into empty vials several times during the course of two days to rid the surface of their eyes from any debris that might have been present in the vials they hatched in. Next, the flies were incubated on a shaker for 2hr at RT in a fixative containing, 1% gluteraldehyde, 1% formaldehyde, 0.1M sodium cacodylate pH 7.4 and a drop of Triton X-100 (to decrease surface tension so the flies will stay submerged). The fixative was then removed and the flies were put through a series of ethanol dehydrations in order to remove water from the tissues. Incubations were 4-12hr for each ethanol concentration at RT on a shaker using the following ethanol series: 25% once, 50% once, 75% once and 100% twice. Following the second 100% ethanol dehydration the flies were sputter coated by the UD Bioimaging Center and sputter-coated in order to be visualized by SEM.

2.9 ***alg10*** **Eye Clones**

In order to generate *alg10* null eyes, a *GMR-hid* system was used in order to select for mutant tissue in the developing eye. To do this, virgin females of the genotype *eyflp/eyflp;sen-gal4/Cyo;GMR-hidFRT*^{2A}*/TM6B,Tb* were crossed to *alg10-10FRT*^{2A}*/TM3,Sb* males in order to generate *alg10* null eyes. By crossing *eyflp/eyflp;sen-gal4/Cyo;GMR-hidFRT*^{2A}*/TM6B,Tb* virgin females to *w/+; FRT*^{2A}*FRT*^{2B}*/TM3,Sb* males, a WT *alg10* eye could be obtained. The principle here is that GMR is specifically expressed in the eye to induce homologous recombination to generate either +/+ eyes or *alg10/alg10* eyes in response to Flp expression in the *eyeless* domain. These are the only two possible viable genotypes that can result since *hid* segregates with GMR. Since *hid* is a dominant, pro-apoptotic gene, the presence of *hid* in tissues that fail to undergo homologous recombination ensures that these tissue are never allowed to develop.

Chapter 3

RESULTS: PHENOTYPIC CHARACTERIZATION

3.1 Zygotic Lethal Phase Determination

Examination of the collection plates for unhatched embryos yielded 21%, 23% and 28% lethalities for the experiment when performed in triplicate. This corresponds to an overall average percent lethality of 24.7% for the experiment. Since 25% of the embryos resulting from the cross were expected to be homozygous for the *alg10* mutation and 100 total flies were used in each experiment, a 25% lethality would indicate that all of these homozygous mutant flies died during embryonic development. Since we obtained 24.7% this tells us that essentially all of the embryos homozygous for the *alg10* mutation die during development. This indicates that *alg10* is an embryonic lethal mutation and proper Alg10 function is critical for normal *Drosophila* embryonic development.

After confirming that Alg10 function is vital for *Drosophila* development, it then became of great interest to test for developmental processes that might be disrupted by Alg10 loss of function. Upon staining the CNS of the embryos from this experiment with a FasciclinII (FasII) antibody, developmental defects of the nervous system were immediately noted (Fig. 12). What is observed in WT embryos is that the fascicle bands appear very evenly spaced apart from one another. In addition to this even

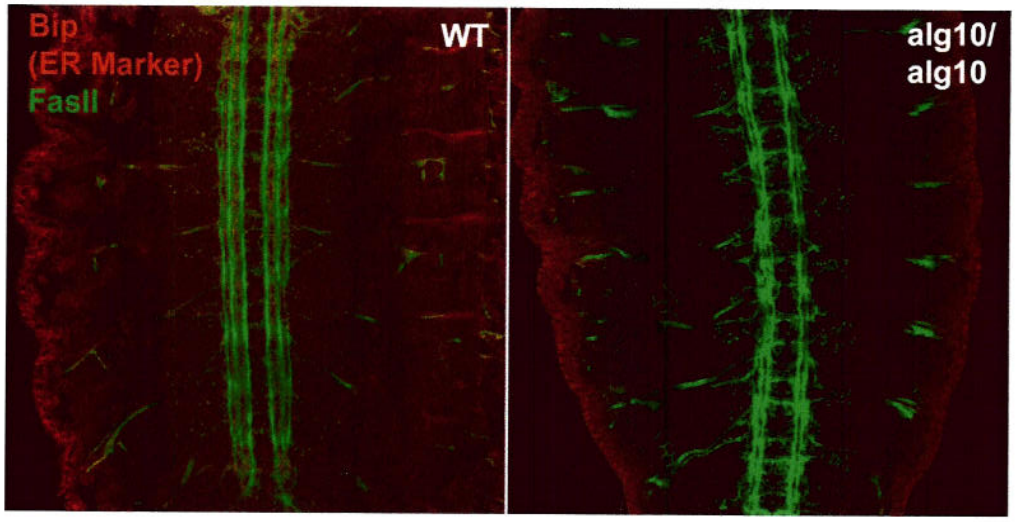

Figure 12: *alg10* zygotic lethal phenotype. When stained for Bip (red) and FasII (green) expression, WT embryos appear to have evenly-spaced fascicle bands whereas the intermediate and lateral fascicles of the *alg10/alg10* embryos appear aggregated indicating defective CNS development.

spacing of fascicle bands, there is slight neuronal crossing-over of the midline as is characteristic of WT embryos. What one notices in the homozygous mutant embryos, however, is an immediate defect in fascicle spacing. The spacing between the medial fascicles appears to be comparable to WT, but the spacing between intermediate and lateral fascicles is abolished, as they appear very condensed and aggregated. In addition to this aggregation, much more excessive crossing-over of the midline is observed in the homozygous mutant embryos than WT. All in all this indicates that not only is Alg10 function important for organismal development in general, but also nervous system development more specifically.

3.2 Germline Clones

Examination of the germline clone embryonic cuticles prepared from homozygous mutant *alg10* embryos provided some degree of insight as to what was going on during the development process. As can be seen from Figure 13, a very pleiotrophic phenotype was observed. Pleiotrophic here is taken to mean that several developmental processes appear to be disrupted by loss of Alg10 function. One will note that as compared to the wild type

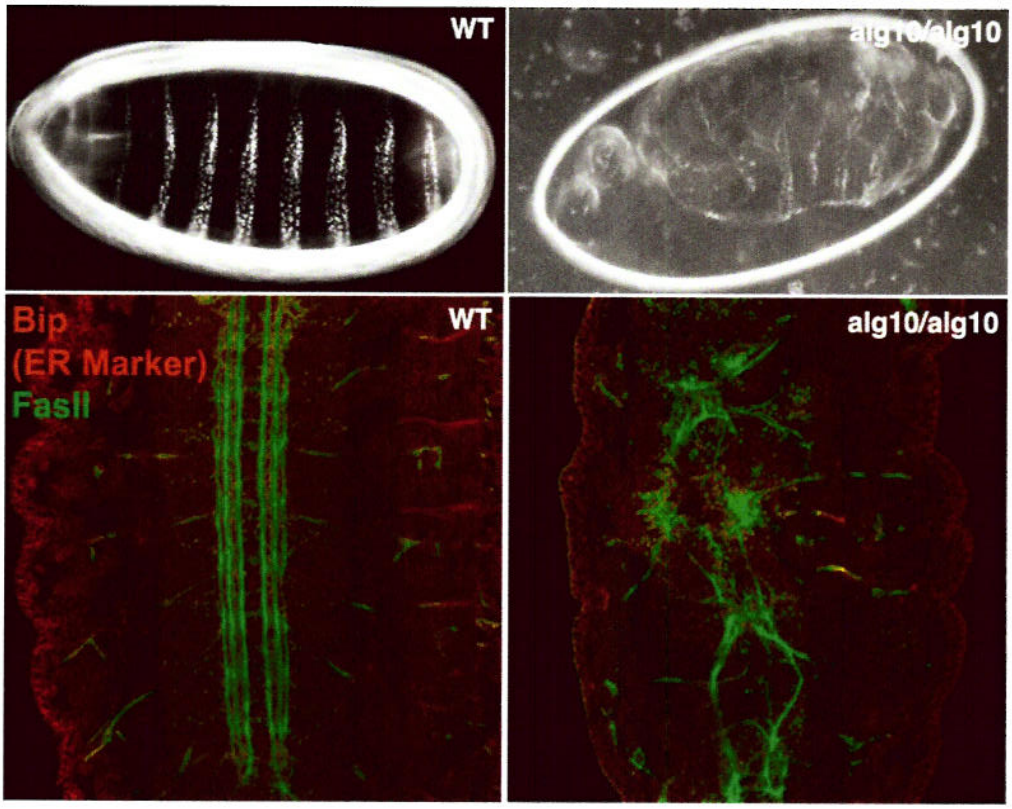

Figure 13: *alg10* germline clone phenotype. Composite showing *alg10* loss of function effects in developing *Drosophila* embryos. (top left) Wild type embryonic denticle phenotype reflecting proper segmentation, (top right) *alg10/alg10* homozygous mutant embryos displaying pleiotrophic loss of function phenotype, (bottom left) WT embryo stained for Bip (red) and FasII (green) showing previously seen fascicle band pattern, (bottom right) true *alg10* loss of function phenotype in absence of maternal component.

reference embryo, there appears to be complete abolishment of denticle bands along the entire length of the *Δalg10/Δalg10* mutant embryos. Since these denticle bands arise as a result of morphogen signaling gradients, this would suggest that Alg10 is important for signaling events required for the differentiation of these structures.

Furthermore, there appears to be substantial nervous system patterning and development defects present. This defective nervous system formation is particularly manifested in the anterior portion of the mutant embryos where the heads of the developing flies appear to be very crumpled and by no means comparable to wild type. The remainder of the embryos prepared along with the cuticles will be used in subsequent immunohistochemical stainings to determine exactly what molecular processes are disrupted at given times during embryonic development.

The severity of developmental defects was further confirmed by staining with FasII, as in the prior zygotic loss of function study (Fig. 13). Again, the same WT patterning was seen when staining with FasII was performed, however the germline clone *alg10* loss of function phenotype seen here in absence of the maternal component is much more profound. When homozygous mutant embryos are stained with FasII they appear severely developmentally defective for nervous system development and CNS patterning. In fact, the CNS looks like it explodes, displaying critical neuronal spacing and pathfinding defects throughout. This study further confirms the zygotic loss of function experiment by also demonstrating that

Alg10 function is required for development of proper morphology and proper nervous system wiring.

3.3 Antibody Staining in Larval Clones

Since Wg is a known glycoprotein that must be properly glycosylated in order to ensure its ability to signal properly, antibody staining in larval wing disc clones for Wg expression was performed. Upon examination, the resulting discs yielded a Wg expression pattern that exactly duplicates WT Wg expression. In particular, in the patches of homozygous mutant clonal tissue generated Wg signaling – as well as other components of Wg and Hh signaling (data not shown) – appears completely unaffected (Fig. 14). This result of a known glycoprotein signaling properly in homozygous mutant tissue was initially very surprising, but will be given much more careful consideration in the discussion.

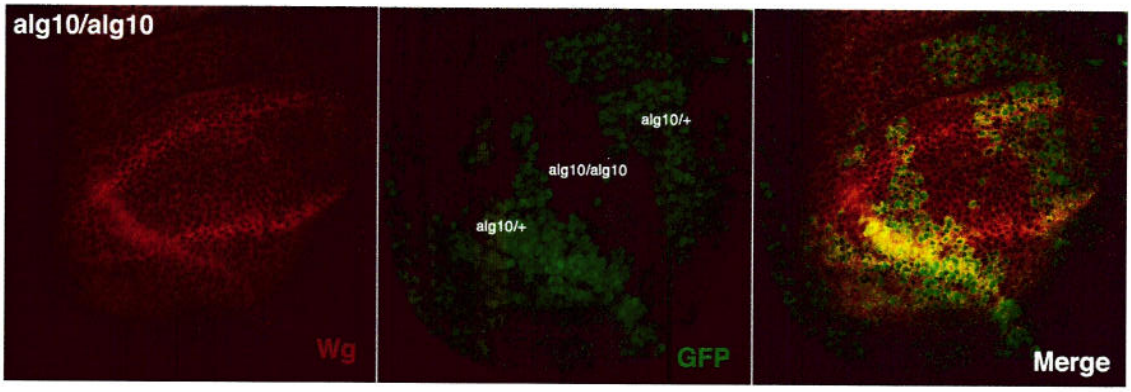

Figure 14: Imaginal wing discs stained for Wg expression. Composite showing Wg staining of *alg10* mutant wing discs. Wg expression is shown in the left panel, GFP expression marking heterozygous vs. homozygous mutant tissue in the middle and the overlay in the right panel showing Wg expression among heterozygous vs. homozygous mutant tissue.

3.4 Adult Wing Clones

In order to understand exactly which pathways might be getting disrupted by loss of *alg10* function during development, adult wing clones were generated. This experiment is essentially the same experiment as our larval clone experiment, except the clones generated are unmarked. The end fate of the clones is not immunohistochemical staining, but rather gross phenotypic analysis.

Examination of the adult wings that were generated yielded a very subtle, yet discernable, phenotype (Fig. 15). As compared to WT wings, the *alg10* mutant wings appeared to be both 10% shorter and rounder. While the mutant wings appeared both shorter and rounder compared to WT wings, the key observation made was that direct comparison of WT and mutant wings showed conservation of wing vein patterning.

Figure 15: *alg10* adult wing clone phenotype. Composite showing WT (left) vs. adult *alg10* mutant clones generated. Note the 10% (n=26) shorter and rounder character of the mutant wing as compared to WT, yet the conservation in wing vein patterning.

This obeservation helped narrow the search for putative disrupted pathways, as only two pathways in *Drosophila* are known to control wing growth in such a manner so as to preserve wing vein patterning yet alter total

organ size. These two pathways are the InR/PI3K pathway and the EGF/myc pathway. Based upon preliminary phenotypes found in the literature, the InR/PI3K pathway appeared to give rise to phenotypes that more closely corresponded with what was observed in the *alg10* adult clone experiment. Thus, the InR/PI3K pathway was selected as the first candidate pathway for investigation.

3.5 Alg10-InR/PI3K Genetic Interaction Study

Since the InR/PI3K pathway was selected as the primary candidate for disruption, a genetic interaction study was performed to see if a genetic interaction actually existed between *alg10* and the InR/PI3K pathway. Since the InR is a known glycoprotein and an ideal place to study InR signaling in *Drosophila* is in the eye, constitutive eye-specific InR mutants were obtained for the study. The driving force behind the study was to determine what happens to the activated InR phenotype in a 50% active *alg10* background as compared to a 100% active *alg10* background.

Upon examining WT OR eyes, one will note a very regular patterning of ommatidia across the surface of the eye (Fig. 16A). In addition to the ommatidia being very orderly in their arrangement, they all appeared very uniform in size. Also, one will note that the overall shape of the eye is a smooth curve with no apparent surface disruptions.

Aside from the OR eyes, the middle panel (Fig. 16B) shows the result of crossing *GMR-GAL4/GMR-GAL4;UAS-dInR/UAS-dInR* virgin females to

w^{1118}/w^{1118} males. Moreover, this panel is indicative of the InR signaling phenotype of the constitutive mutants in a 100% active *alg10* background. What resulted was a general disordering of all ommatidia in the eye. In addition to being merely disordered, all of the ommatidia appeared very enlarged in size and even fused together in some places. Apart from the ommatidia, indentations were seen in the overall structure of the eye as compared to the very regular and smooth surface of the WT eye.

Finally, the investigation of InR signaling in a 50% active *alg10* background yielded a phenotype that initially appeared enhanced over the phenotype observed in the 100% active *alg10* background (Fig. 16C). The ommatidia appear very highly fused together as compared to the middle panel, giving the eyes a very glassy look to them. In addition to ommatidial fusion, the overall surface of the eye appeared even more irregular than the 100% active *alg10* eye. Aside from ommatidia and overall eye structure, yellow patches of necrotic tissue appeared throughout the eyes.

In order to investigate the putative enhancement in phenotype caused by 50% knockdown of *alg10* activity as well as to better understand the nature of the necrotic tissue observed, histochemical sectioning of all three genotypes of eyes used in the genetic interaction study was performed. Tangential sectioning of OR eyes confirmed what was seen in the gross phenotypic analysis: the diameter of individual ommatidia in the eye appeared very uniform throughout with little variation and an average ommatidial diameter of 0.116 microns (Fig. 16D, G).

Examination of the constitutive mutant eyes in a 100% active *alg10* background also confirmed what was seen from the initial assessment. The average ommatidial diameter for 56 randomly sampled ommatidia was 0.184 microns (Fig. 16E, G). This corresponded to a 58.6% enlargement of ommatidial diameter, on average, over the OR eyes. In addition to the enlargement of average diameter, the standard deviation showed a marked increase in the variation among individual diameter in the ommatidia sampled.

Aside from the OR and *GMR-gal4/+;UAS-InR-A1325D/+* eyes, sectioning of the *GMR-gal4/+;UAS-InR-A1325D/Δalg10* eyes yielded a slightly different result than expected (Fig. 16F, G.). In the initial assessment, the phenotype appeared enhanced over that of the *GMR-gal4/+;UAS-InR-A1325D/+* flies. However, upon sectioning, a 36.2% overall increase in diameter was observed relative to OR eyes. This corresponded to a 22.4% decrease in ommatidial diameter relative to the *GMR-gal4/+;UAS-InR-A1325D/+* eyes and a suppression in phenotype. Although the decrease in ommatidial diameter observed is not statistically significant relative to *GMR-gal4/+;UAS-InR-A1325D/+* eyes, there is a reduction suggesting a suppression in phenotype.

In order to further address the nature of the origin of phenotype observed in the *GMR-gal4/+;UAS-InR-A1325D/Δalg10* eyes, histochemical staining was performed on transverse sections representing all three genotypes used in the above tangential sectioning study. Examination of the OR eyes yielded sections where the photoreceptor patterning was very smooth and

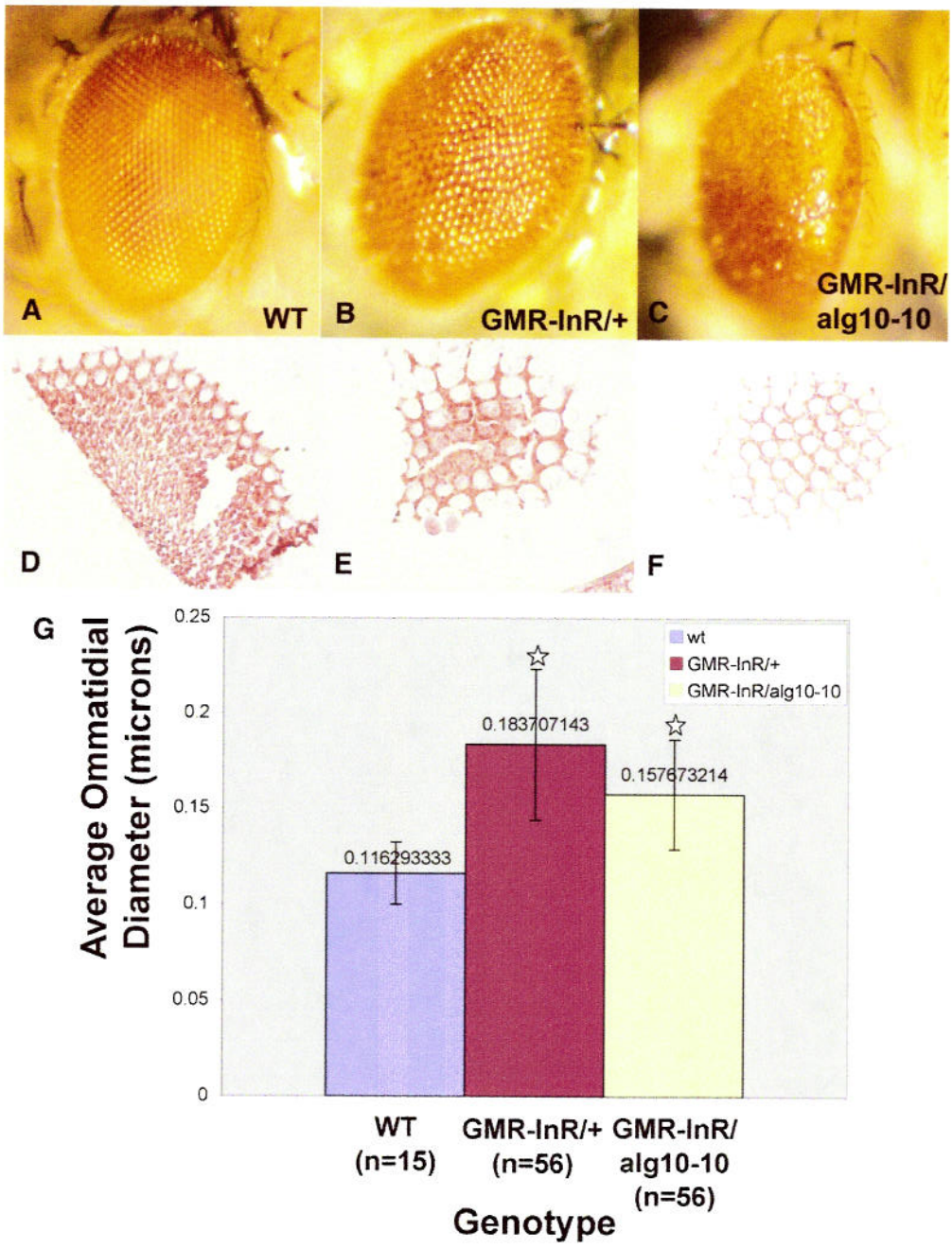

Figure 16: Loss of Alg10 function impairs InR signaling in the eye. (A) very structured and uniform wt OR eye, (B) *GMR-gal4/+;UAS-InR-A1325D/+* eye showing enlarged and disordered ommatidia and uneven eye surface, (C) *GMR-gal4/+;UAS-InR-A1325D/Δalg10* eye showing highly fused ommatidia and patches of necrotic tissue, (D) OR section at 40x, (E) *GMR-gal4/+;UAS-InR-A1325D/+* section at 40x, (F) *GMR-gal4/+;UAS-InR-A1325D/Δalg10* section at 40x showing suppressed phenotype for cell size, (G) Chart showing average ommatidial diameter for all three genotypes as well as variance among ommatidia as reflected by standard deviation.

photoreceptor cell size was uniform with no apparent gaps between photoreceptor cells (Fig. 17). The photoreceptor cells took a very direct path from retina to fenestrated membrane, each finding their proper target.

When the *GMR-gal4/+;UAS-InR-A1325D/+* sections were examined, a definite phenotypic change was noted over the OR eyes (Fig. 17). The photoreceptor cells appeared to be both enlarged and more disordered than those of OR. In particular, one notices large gaps between photoreceptor cells that are not present in the OR sections. Despite these increases in photoreceptor cell size and gaps between photoreceptor cells, all of the photoreceptor axons and cell bodies appear to display connectivity to the fenestrated membrane.

Figure 17: Alg10 loss of function impairs photoreceptor axon guidance. (WT) 20x view showing very regular and uniform OR photoreceptor axon extension, spacing and connectivity, (*GMR-gal4/+;UAS-InR-A1325D/+*) 20x view showing photoreceptor cells that are enlarged in size but still displaying correct target connectivity (*GMR-gal4/+;UAS-InR-A1325D/alg10*) 20x view showing photoreceptor cells suppressed in size, but enhanced in phenotype for axonal guidance defects, displaying semi-frequent connectivity errors and spacing defects between photoreceptor cells.

Apart from the OR sections and the *GMR-gal4/+;UAS-InR-A1325D/+* sections, the *GMR-gal4/+;UAS-InR-A1325D/Δalg10* sections again produced

an interesting story. In analyzing the *GMR-gal4/+;UAS-InR-A1325D/Δalg10* sections, there appears to be several defects in eye development. In these sections there appeared to be both a suppression and enhancement in phenotype taking place. In comparison to the *GMR-gal4/+;UAS-InR-A1325D/+* sections, there appears to be a suppression in phenotype in photoreceptor cell size determination, as the gaps between photoreceptors are greatly minimized and the sections start to look more like OR in general. Despite the fact the photoreceptor cell size may exhibit suppression, an enhancement appeared to occur in photoreceptor cell and axon pathfinding. In the previous instance where *GMR-gal4/+;UAS-InR-A1325D/+* cells and axons appeared to connect properly with the fenestrated membrane, there are several instances in the *GMR-gal4/+;UAS-InR-A1325D/Δalg10* sections where the axons appear to start out from the retina in a correct manner and then veer off course only to never connect to the fenestrated membrane. This lack of connectivity is of great consequence to cell survival and will be further explored in the discussion.

3.6 Adult Eye Clones

Based upon the genetic interaction of Alg10 with the InR signaling pathway, the speculation arose that *alg10* might display a phenotype of its own during eye development. Since global Alg10 loss of function is embryonic lethal, homozygous eye-specific mutants were generated (Fig. 18). This method takes advantage of eye-specific expression of GMR-*hid*, where

hid is a dominant pro-apoptotic gene. This is of consequence, because the presence of *hid* induces apoptosis in the given tissue. Thus, when homologous recombination is induced in *eyflp;sen-gal4;GMR-hidFRT*^{2A}/+ flies, the only viable eye tissue that can be obtained is +/+. Similarly, when homologous recombination takes place in *eyflp;sen-gal4;GMR-hidFRT*^{2A}*/alg10-10FRT*^{2A} flies, the only viable genotype that can be obtained is *alg10/alg10*. Since homologous recombination does not start from the first onset of eye development and not all homologous recombinase sites will be bound, some cells in the developing eye will still be heterozygous for *hid*.

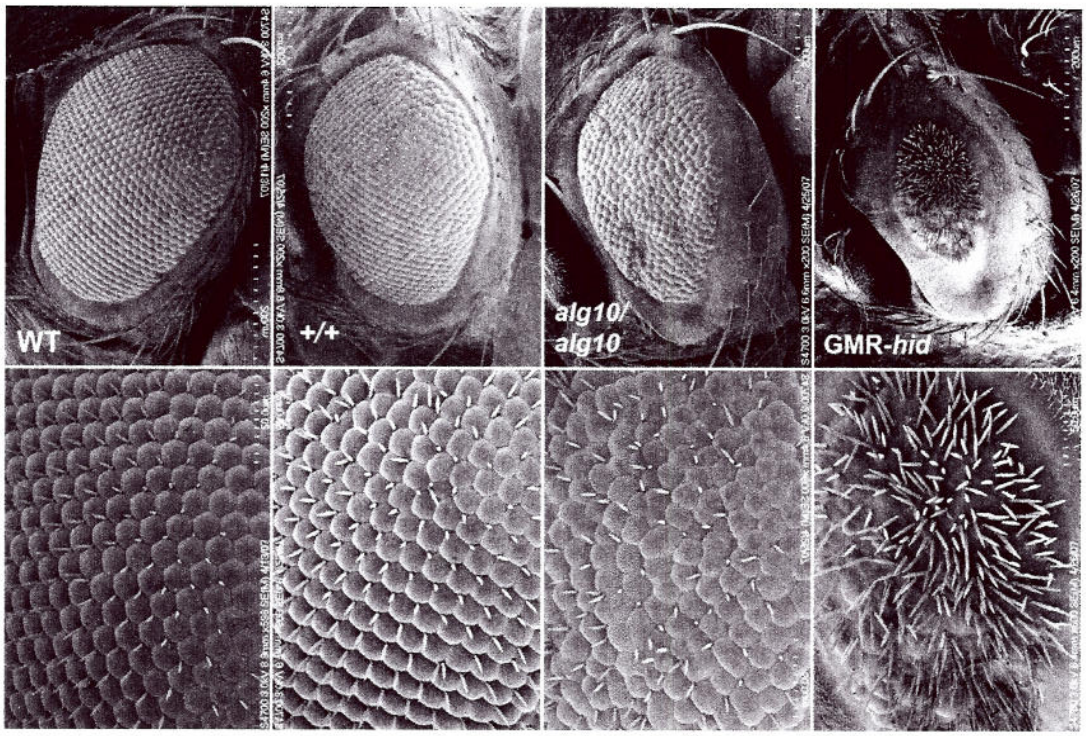

Figure 18: *alg10* null eyes give a rough eye phenotype indicating Alg10 function is important for eye development. Here the same strategy was used as in the adult wing generation, only here the clone tissue generated is specifically in the eye. One addition this approach makes over the wing clone generation is to utilize a GMR-*hid* system where hid is a dominant, pro-apoptotic gene used to preferentially select for homozygous mutant tissue. Thus, the *alg10/alg10* eyes generated are entirely mutant.

This will cause these particular ommatidia to die and is the reason non-uniformity is observed at certain places in the +/+ eye and a pitted surface is observed in the *alg10/alg10* eye. These regions can be distinguished by a high bristle density as is present in the entire GMR-*hid* eye (Fig. 18).

As one can see, the base GMR-hid eye consists of no ommatidia due to global expression of hid which induces apoptosis and kills them. One will note that the presence of bristles is still apparent. This is because bristles and ommatidia are derived from two distinct cell lineages so the presence of hid does not at all impact the cells that give rise to bristles. When the WT chromosome is used in the investigation to generate the +/+ eye used as a basis for comparison, a dramatic rescue is observed where the +/+ eye obtained displays almost a full rescue to WT (Fig 18, far left). Conversely, when a null allele of *alg10* is used, the resulting eye rescues nowhere near the extent of the +/+ eye. Instead, a smaller rough eye phenotype is obtained where ommatidia display slight growth differences, but predominantly fail to form organized lines across the surface of the eye as in the +/+ and WT eyes. This result indicates that Alg10 function is not only important for nervous system development, but also eye development as well.

3.7 Scanning Electron Microscopy of Eyes

When SEM was performed on eyes resulting from the enhancer/suppressor study conducted, several things were noted. As an overview, components of the InR pathway as well as different *alg10*

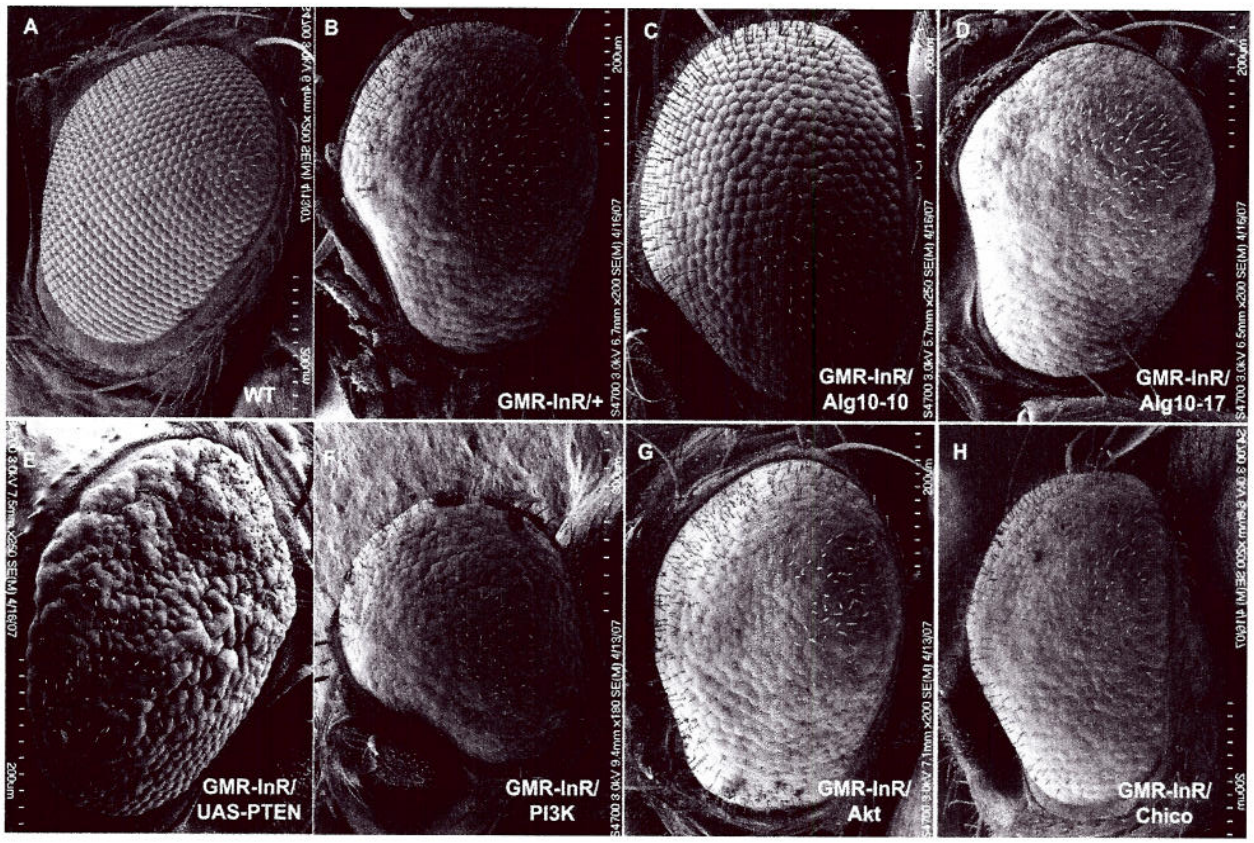

Figure 19: SEM of eyes used in the Alg10-InR pathway enhancer/suppresser study. Various components of the InR signaling pathway along with *alg10* were used in crosses with an eye-specific constitutive InR background to evaluate their ability to enhance or suppress the GMR-InR/+ phenotype. (B) *GMR-InR/+*, (C) *GMR-InR/alg10-10*. (D) *alg10-17*, (E) The UAS-PTEN, (F) dominant negative PI3K, (G) Crossing in constitutively active copies of *Akt* and (H) *Chico*.

mutations were used in crosses to place them in a constitutively active, eye-specific InR background (Fig. 19). Based upon the nature of the interaction (if any) an enhancement or suppression in phenotype is expected to occur. When *GMR-InR/alg10-10* is used, a suppression in phenotype is observed where the overall eye appears 18.8% narrower (Anterior → Posterior) and 22.9% shorter (Dorsal → Ventral) relative to GMR-InR/+ and patterning starts to resemble WT to a much higher degree. Some ommatidia growth effects are noted, but as reflected from the tangential sectioning, the nature of the phenotype is likely due

more to proliferative effects. The use of *alg10-17* yields an eye that very closely resembles the *GMR-InR/+* eye, which indicates that this allele is probably a weak mutation in *alg10*. The UAS-PTEN mutant shows a very enhanced phenotype, however it is the only UAS line used in this investigation. Consequently, UAS-mediated overexpression presents one with a different basis of comparison relative to other genotypes utilized in this study. Thus, the experimental value of this particular cross is low and should be disregarded. Using a dominant negative PI3K or a *Chico* loss of function appears to yield significantly smaller eyes for both proliferation and ommatidial size. Lastly, using a constitutively active form of the positive regulator *Akt* causes an enhancement in phenotype for proliferation.

Chapter 4

DISCUSSION

4.1 Conclusions

These results have led to the following three conclusions: 1) Alg10 displays a genetic interaction with at least the InR/PI3K Pathway to modulate proper growth control during *Drosophila* development, 2) Alg10 function is critical for normal *Drosophila* growth and development and 3) Regulation of Glycosylation is likely to be involved in cellular growth control.

4.1.1 Alg10 displays a genetic interaction with at least the InR/PI3K pathway to modulate proper growth control during *Drosophila* development

Results from the adult clone generation strongly supported the notion that the InR/PI3K pathway and/or the EGF/myc pathway were disrupted in tissue homozygous for the *alg10* mutation. Since only these two pathways govern wing growth in such a manner as to alter total organ size while preserving wing patterning, it is likely one or both is/are disrupted. While the EGF/myc pathway may indeed be disrupted, disruption of the InR/PI3K pathway was confirmed in this work. The investigation of EGF/myc disruption will be left for future studies. Confirmation of InR/PI3K disruption was verified in the eye-specific studies performed where the presence of a constitutively active InR in a 50% active Alg10 background produced a

dimorphic phenotype that appeared suppressed for cell growth, yet enhanced for axonal guidance defects relative to the constitutively active InR in a 100% active Alg10 background [37,38,39].

4.1.2 Alg10 function is critical for normal *Drosophila* Growth and Development.

Taking into account the results of the zygotic lethal phase and germline clone experiment, the conclusion can be drawn that Alg10 function is absolutely critical for organism viability through development. More specifically, having a fully glucosylated core sugar substrate is – at least in some tissues such as nervous tissue – vital for ensuring proper development. The zygotic phenotype experiment showed that the *alg10* mutation is an early embryonic lethal mutation, indicating Alg10 function is required early in development. Since Alg10 function is required so early in development, an important fundamental process is likely to be disrupted.

In light of the pleiotrophic germline clone phenotype observed, several developmental processes appear to be disrupted. This is not terribly surprising considering that approximately 70% of all secretory proteins are predicted to bear some kind of N-glycosylation and the specific catalytic STT3A-containing OST isoform is known to be localized to highly secretory tissue such as the liver and pancreas which contain unusually large amounts of rough ER [20]. While it has not been molecularly confirmed, the suggestion that neurons express the STT3A isoform is not unreasonable. Neurons are a

highly secretory cell type that contain a large amount of rough ER as well as a noticeably large nucleolus, indicating high ribosome production and hence, a high degree of protein synthesis [46]. This would be of consequence because in highly secretory or nervous tissue lacking Alg10 function, glycosylation could not take place because the STT3A isoform will not transfer sugar substrates lacking the glucose put on by Alg10.

Thus, proteins that must be glycosylated in order to function properly will not be glycosylated and most likely not be able to fold properly. If the protein is still able to fold, the likelihood that it will be able to carry out its native function or be targeted properly is small. Despite a pleiotrophic phenotype being observed, nervous system development and patterning appears to be specifically impaired. The immunohistochemical staining performed against the CNS marker FasII in the zygotic *alg10/alg10* embryos demonstrated a requirement of Alg10 function for proper nervous system development. In these embryos homozygous for the *alg10* mutation, aggregated intermediate and lateral fascicles were observed along with excessive neuronal crossing over of the midline. However, staining of the germline clone *alg10/alg10* embryos confirms the fact that Alg10 function is needed for proper nervous system development even more dramatically, as axonal guidance appears to be severely disrupted by loss of Alg10 function.

In addition to the zygotic phenotype and germline clone experiments, the sectioning and histochemical staining provides further compelling evidence that nervous system development is disrupted. InR expression is

known to be required during development for proper axonal guidance from the photoreceptor retina to its target tissue on the brain. What was observed in the *alg10* mutant eyes is an enhanced phenotype for axonal guidance but a suppressed phenotype for ommatidial and photoreceptor cell size. The suppression in cell size was confirmed nicely through the tangential sectioning and SEM performed. While the gross suppression in eye phenotype looked much clearer in the SEM pictures of *GMR-InR/alg10-10* eyes, a less-dramatic suppression in average ommatidia diameter was observed from the statistical analysis of the tangential sections taken. It is likely that a much more significant suppression actually exists, but many more tangential sections would need to be taken to obtain a larger sample size in order to establish statistical significance. Both the enhancement and suppression make sense given the fact the InR is known to be heavily N-glycosylated, as suppressing the function of a positive regulator of growth will cause decreased cell growth and suppressing the function of a positive regulator of axonal guidance will result in an enhancement of axon guidance defects.

The results obtained for the dominant negative PI3K, *Chico* mutant and constitutively active *Akt* are as expected. Since PI3K-Akt signaling regulates InR and 4EBP transcription to govern proliferation through FOXO and TOR signaling functions to mediate changes in cell growth, respectively, taking away a positive transcriptional regulator that primarily governs proliferation is likely not going to have much of an effect on cell growth. The exact link between PI3K and TOR signaling to mediate changes in cell growth

is poorly understood, but it is likely that induction of TOR signaling can be stimulated in a PI3K-independent manner such that the reduction in organ size should be confined primarily to proliferative effects due to lack of active PI3K (45). Indeed, a smaller eye results with minimal effects apparent on cell growth, indicating that effects on proliferation appear to be what gives rise to the observed phenotype. In addition, *Chico* loss of function appears to have a similar effect. Regarding *Akt*, expression of a positive regulator of growth should have little effect on the extent of cell growth observed in a constitutively active InR background since maximal activation of growth control via the InR is already occurring. Indeed, what is observed in *GMR-InR/Akt* eyes closely resembles what is seen in the *GMR-InR/+* eyes. These studies seem to show that *alg10* is acting as a positive regulator of InR signaling to primarily mediate proliferation and to lesser degree cell growth, which is consistent with the histochemical sectioning performed.

In addition to the fact that the InR is heavily glycosylated, it is the only component of the InR/PI3K pathway known to bear the modification of N-glycosylation. The defects observed in axonal guidance coupled with a genetic link between *alg10* and the InR/PI3K pathway suggest defective glycosylation of the InR in homozygous mutant *alg10* tissue. The *alg10/alg10* germline clone phenotype lends further credence to the likelihood that axonal pathfinding is disrupted, as without Alg10 function fascicle bands fail to achieve WT patterning. Further molecular experiments will be required to verify defective glycosylation of the InR with complete certainty, but it is

an extremely likely target. If the InR is in fact aberrantly glycosylated, it will either a) not properly fold, b) not be incorporated properly in the cell membrane or c) be incorporated into the cell membrane but not be capable of undergoing a productive ligand interaction. In either case, the consequence is having a lack of InR/PI3K signaling in nervous and secretory tissue which should phenocopy the axonal guidance defects observed in $InR^{-/-}$ embryos.

As previously mentioned, a suppression in ommatidial growth can also be explained by decreased glycosylation of the InR. Since chief downstream effects of InR signaling are protein synthesis and cell growth, a physical lack of cell-surface InR would impose a critical block in maintaining cell growth. In the genetic interaction study, *GMR-gal4/+;UAS-InR-A1325D/Δalg10* mutants generated are heterozygous for the *alg10* mutation. Thus, it makes sense that a partial supression would occur with variation in ommatidial diameter still present, as 50% of Alg10 activity still remains in order to maintain cell growth to a certain degree. This trend is reflected by the decrease observed in average ommatidial diameter between *GMR-gal4/+;UAS-InR-A1325D/+* and *GMR-gal4/+;UAS-InR-A1325D/Δalg10* animals.

4.1.3 Regulation of Glycosylation is likely to be involved in cellular growth control

Accounting for all of the data, one cannot help but note a dichotomy between the results of the Wg staining in the larval clone wing discs and the

results of the germline clone cuticle phenotype. It is evident that something must be going on molecularly to mediate proper glycoprotein signaling in the wing disc despite lack of Alg10 function in the homozygous clone tissue. In addition, global lack of Alg10 function in the developing embryo cannot be tolerated as is evidenced by the strong embryonic lethal phenotypes observed. This observed dichotomy is likely to be explained by tissue-specific expression of specific and nonspecific OST isoforms. Without verifying this through co-localization studies it is hard to say with complete certainty, but it is likely that in tissues like the wing disc where secretory demand is lower the nonspecific STT3B isoform is present to rescue lack of Alg10 function. Conversely, in places like the medial Neurosecretory Cells (mNSCs) where *dilps* originate and secretory demand is high, it is likely that the STT3A isoform is present to ensure 100% correct glycosylation of developmental components all of the time.

Since the axonal guidance defects and suppression in cell size point to a lack in glycosylation of the InR, this raises the intriguing possibility that *alg10* is regulated under normal developmental circumstances in order to help in mediating growth control. If the mNSCs display a lack of InR glycosylation (and thus a lack of active cell surface InR), cell size will decrease. This should, in turn, decrease net secretion from the cells. Since the mNSCs are the origin of *dilp* expression in *Drosophila*, *dilp* expression into the circulation is likely to decrease [32].

In the context of a homozygous *alg10* mutant organism, glycosylation could still take place in tissues where the nonspecific isoform is expressed so *dilp* signal reception on target cells could still take place and growth could occur. However, a problem is posed for the nervous system where a lack of active cell surface InR is present, rendering InR/PI3K signaling impaired. This impairment in InR/PI3K signaling reduces PI3K activation via Chico in *Drosophila*.

Since PI3K phosphorylates many vital cell regulators, it is not out of the question to speculate that one such regulator could be a positive regulator of the *alg10* gene. Indeed, microarray analysis performed with human DNA has shown that a downstream target whose expression is activated by insulin is *alg10* [40] (Appendix). Depression of any positive regulator of the *alg10* gene will decrease its transcription, decreasing the level of active Alg10 in the lumen of the ER. For example, during prolonged insulin stimulation IRS-1 and 2 are known to be selectively targeted for degradation by the ubiquitin-proteasome system [41], which would work to decrease *alg10* transcription. This positive regulator depression would be critical in regulating growth control in STT3A-expressing tissue, as not only does this decrease InR glycosylation by halting the terminal step of N-glycosylation, but it provides nutritional refinement by increasing the cytoplasmic pool of UDP-glucose (UDP-Glc).

Due to the fact that Alg10 is a glucosyltransferase and sugars are transported to the ER as nucleotide activated sugars, this increase in the

cytoplasmic pool of UDP-Glc is logical. Being that intracellular sugar pools are carefully regulated in order to limit the wasting of energy, this pool of UDP-Glc is likely to be an important nutritional regulator. An increase in this pool would cause the levels of the UDP-Glc precursor, glucose-6-phosphate (Glc-6-P) to increase. Interestingly, Glc-6-P is the precursor for the biosynthesis of both UDP-GlcNAc and GDP-Man, the other two main sugars used in the biosynthesis of the core oligosaccharide structure for N-glycosylation [13,14]. This is of note, because the steps requiring UDP-GlcNAc and GDP-Man all precede the three terminal steps that require UDP-Glc. Thus, if Glc-6-P levels increase and there is a lesser demand for UDP-Glc, this would actually shunt the biosynthesis of nucleotide activated sugars more toward UDP-GlcNAc and GDP-Man, allowing more core oligosaccharide biosynthesis to take place up until the Alg10-requiring step. In places like the nervous system, this is of interesting consequence, as having an abundance of immature core oligosaccharide in the lumen of the ER awaiting Alg10 function would enable an especially rapid response to induction of Alg10 activity following *dilp* stimulation. An increase in Glc-6-P levels is likely to cause an increase in intracellular Glc levels since Glc is the immediate precursor to Glc-6-P. This increase in Glc will both feed back on the glucose transporter to decrease the amount of glucose being imported into the cell as well as be channeled into glycolysis in attempt to restore glucose levels [42].

Also of note is that there are no known homologs of mammalian glucagons in *Drosophila*. Thus, the question of how gluconeogenesis is regulated comes into play. In mammalian systems the site of gluconeogenesis is the liver, whereas in *Drosophila* it occurs in the fat body. Since liver tissue is known to preferentially express the STT3A OST isoform, it is reasonable to conclude that the fat body in *Drosophila* does as well. This could establish a mechanism in insects whereby the depression in active Alg10 levels due to starvation would cause an increase in the pool of UDP-Glc, which in turn causes increases in the levels of Glc-6-P, Frc-6-P and Glc itself. The key thing is that both Glc-6-P and Frc-6-P are intermediates for gluconeogenesis, so they can be directly metabolized in order to provide Glucose for the organism. Since Phosphoglucose Isomerase is also a glycolytic enzyme, this induction of its activity to catalyze the coversion of Frc-6-P → Glc-6-P could then potentially feed back on glycolysis to channel pyruvate into the gluconeogenic pathway.

The key feature of this model is that it provides a mechanism for rapidly modulating active glycoprotein levels where *alg10* might serve as a master regulator of cell secretion. While it is hard to predict the impact loss of glycosylation would have on minimally glycosylated proteins (those having only one or a few glycosylation sites), one can say with a better degree of certainty that levels of active heavily glycosylated proteins (ones where glycosylation is absolutely critical for function, such as the InR) are likely to be modulated in response to both nutritional and developmental cues in the

form of *dilps* in *Drosophila*. In mammals the story is likely to be much the same, only with added players. In *Drosophila*, all of the *dilps* signal through one insulin receptor with one adaptor (Chico). This serves to activate one kinase (PI3K) in order to regulate *alg10* and hence, active InR levels. Furthermore, there are only two isoforms of OST in *Drosophila*.

In mammals, an InR exists with a variety of adaptors (IRSs) along with various IGFRs all of which have their own downstream kinases targets which could all converge in determining net *alg10* activation. Thus, in mammals, there is more likely to be this averaging effect that is the result of signaling through multiple growth receptors. In addition to multiple growth receptors, mammals possess more catalytic OST isoforms than insects, which is likely to result in the ability to fine tune intracellular pools of UDP-Glc to different degrees. This makes logical sense given the fact mammals require a higher degree of tissue-specific growth control than do insects.

4.2 Future Work

4.2.1 Genetic Interaction with Additional InR/PI3K Path Components and EGF/c-myc Pathway

As previously mentioned, the EGF pathway is a likely candidate for disruption besides the InR pathway because it is known to regulate wing growth in a manner consistent with our observed *alg10* mutant phenotype. In addition to being consistent with our wing growth phenotype, a further case is

made for EGF disruption due to the result of the transverse sectioning that was performed. EGF signaling is known to be a key player in eye development, specifically in R8 cell spacing and non-R8 photoreceptor cell differentiation [43, 44]. Interestingly, photoreceptor cell differentiation starts with R8 and all subsequent photoreceptor cells need R8 signaling at a very precise time during development in order for proper differentiation. This necessity arises because the R8 cells are the predominant source of Spitz in the eye during development which, along with gurkin and kekkon, is the ligand for the EGFR.

What is even more interesting, however, is that Spitz is known to be extensively O- and N-linked glycosylated. The N-glycosylation of Spitz is of consequence in *alg10* mutant photoreceptor cells, as they will lack this modification. Whether this lack in N-glycosylation would hinder Spitz from folding in the first place or prevent its downstream association with Star for intracellular transport has yet to be determined, but is likely to result in the disruption of Spitz's ability to signal.

The investigation of genetic interaction of *alg10* mutants with components of the EGF pathway needs to be carried out as was done with the InR/PI3K pathway. Furthermore, clones in the eye disc should be generated and examined for active Spitz expression using immunohistochemical staining to molecularly confirm whether disruption in Spitz signaling correlates with Alg10 loss of function. This confirmation would prove very useful in

rendering a more complete interpretation of the *alg10* loss of function eye phenotypes we observe for components of the InR pathway.

4.2.2 Probing the Alg10 Loss of Function Phenotype with Hairpin RNAi

During the course of future investigations the need will arise to make use of the hairpin RNAi constructs that I generated in my work here. A hairpin construct against *alg10* as well as an *alg10* cDNA rescue construct was generated in this investigation. Control hairpin constructs against Wingless (Wg) and Porcupine (Porc) were also synthesized. These constructs will ultimately be used to make transgenic lines by embryo microinjection. Once transgenic lines are obtained, loss of function studies can be conducted at select points in development since the transgenes were placed under control of a heat shock-inducible or tissue-specific promoter.

The attempt here is to recapitulate *in vivo* the *alg10* embryonic loss of function phenotype observed in the germline clone experiment. By crossing our *UAS-alg10* hairpin or a line bearing the *UAS-alg10*cDNA to a tissue-specific Gal4 driver line, such as GMR-gal4 used in these studies, it can be determined whether overexpressing *alg10* rescues the loss of function phenotype and whether RNAi targeting of *alg10* recapitulates the *alg10* loss of function phenotype observed *in vivo*. This will unambiguously show that the phenotypic effect is *alg10* specific.

4.2.3 Southern Blots of *alg10* Deletions to Confirm Null Mutations

The deletions generated for use in this investigation have only been preliminarily confirmed by way of DNA PCR analysis. Thus, it will prove informative to do diagnostic Southern blots in subsequent studies in order to confirm the nature of the *alg10* deletions. As previously mentioned, the deletions should abolish much of the 5' regulatory portion of the *alg10* gene, so the mutations are assumed to be null mutations. However, probing Southern blots will allow us to physically see that the deletions would be expected to give rise to no active gene products.

4.2.4 Germline Clone Generation to Stain for Unfolded Protein Response (UPR) Activation and Markers For Tissues Requiring Alg10 function

The germline clone experiment must be repeated in order to generate more homozygous mutant *alg10* embryos that can be prepared for immunohistochemical staining. This will be performed for two reasons: in order to examine any tissue-specific activation of UPR and to molecularly examine nervous system development in the context of a homozygous mutant embryo. By staining for UPR markers, this will give direct insight into

whether there is a block in glycosylation, as unfolded proteins should accumulate in the ER in these tissues.

In addition to merely confirming a block in glycosylation, it will allow tissue-specific assessment of UPR upregulation. The staining of nervous system markers will supplement the UPR upregulation study and allow determination of the extent of disruption on a global developmental scale. Thus, seeing a lack of glycosylation and upregulation of UPR in nervous tissue would be consistent with phenotypic effects observed in this investigation and suggest unfolded InR (and other proteins where N-glycosylation is essential for folding) as a result of *alg10* loss of function.

4.2.5 Co-Localization of Alg10 Expression with STT3A and STT3B Isoform Activity

While the proposition has been put forth that there exists a tissue-specific expression pattern of the OST STT3A and STT3B isoforms, this needs to be confirmed on the molecular scale in order for the proposed model to be validated. Thus, co-localization studies need to be performed in order to confirm that, in fact, the specific STT3A isoform is localized to nervous and highly secretory tissue along with a lack of Alg10 function. By observing STT3A localized to nervous tissue where a lack of Alg10 function is present, the statement can confidently be made that N-glycosylation of glycoproteins will be impaired due to the inability of the specific isoform to recognize a hypoglucosylated substrate. This result will greatly help in elucidating a

molecular confirmation of the observed germline clone phenotype where on a gross phenotypic scale, nervous system development appears to be impaired.

4.2.6 *alg10* Transcription Factor Profiling

Since transcription factor profiling has not been performed for *alg10*, it is of great interest to see how exactly this gene is regulated. Previously mentioned was the fact that it is known that insulin binding to the InR causes *alg10* activation, but the steps in between receptor activation and transcriptional activation have not been examined. Thus, conducting a transcription factor profiling experiment using the *alg10* promoter as well as a large portion of the 5'UTR of *alg10* as bait would be of great interest. By incubating this immobilized DNA with nuclear extracts and crosslinking the subsequent DNA-protein complexes, one can obtain a profile of any transcription factors that may bind to regulate *alg10* expression.

4.2.7 *In situ* Hybridizations to Assess *dilp* Expression in *alg10* Mutant Germline Clone Embryos

Performing *in situ* hybridizations will be telling for a couple of reasons. First of all, it allows one to visually assess where gene products are being made and in what amounts in organisms. Since the *in situ* procedure is technically demanding, antibodies are often favored for this task. However, *in situ* hybridization is utilized because few proteins have antibodies that work *in situ*. Some may have proteins made, but only display certain species

reactivity. Thus, antibodies that fall into this category would not be of any kind of experimental use in the investigation. The *dilps* in *Drosophila* happen to fall into the latter category of having no antibodies around to readily stain for them. However, there is an established record of *dilp* expression from a wild type *in situ* used in attempt to understand where each *dilp* is expressed during development [22]. Thus, following a similar protocol for *alg10* germline clone embryos, the dependency of *dilp* expression on Alg10 function during development in different tissues can be readily observed on a global scale.

REFERENCES

1. Hartwell, L. H., Hood, L., Goldberg, M.L., Reynolds, A.E., Silver, L.M., Veres, R.C. (2004). Genes: From Genes to Genomes. New York, McGraw Hill.

2. Kane, K. (2007). "CBIO341: Introduction to embryology." from http://www.mc.vanderbilt.edu/devbio/2007mdbmodule1.html.

3. Purves, e. a. (1995). Life: The Science of Biology. Gordonsville, VA, W.H. Freeman.

4. Sullivan, W., e. a. (2000). Drosophila Protocols. Cold Spring Harbor, New York, Cold Spring Harbor Laboratory Press.

5. Staveley, B.E. (2007). "Developmental Biology (BIOL 3530)." From http://www.mun.ca/biology/desmid/brian/BIOL3530/DB_Ch02/DBNModel.html.

6. Roberts, D. B. (1986). "Basic *Drosophila* care and techniques. In *Drosophila: A Practical Approach*." (ed. D.B. Roberts): 1-38.

7. Sturtevant, M. A. and E. Bier (1995). "Analysis of the genetic hierarchy guiding wing vein development in Drosophila." Development 121(3): 785-801.

8. Selva, E. M. and Stronach, B.E. (2007). Germline clone analysis for maternally acting *Drosophila* Hedgehog components. Molecular Methods in Molecular Biology: Hedgehog Signaling: 129-144 (in press).

9. Oh, S. H., et. al. (1992). "Modulation of calmodulin levels, calmodulin methylation, and calmodulin binding proteins during carrot cell growth and embryogenesis." Archives of Biochem. and Biophys. 297(1): 28-34.

10. Alberts, B., et al. (2002). Molecular Biology of the Cell. New York, Garland Science.

11. Abramsson, A., et. al. (2007). "Defective N-sulfation of heparan sulfate proteoglycans limits PDGF-BB binding and pericyte recruitment in vascular development." Genes Dev. 21(3): 316-331.

12. Burda, P. and M. Aebi (1999). "The dolichol pathway of N-linked glycosylation." Biochimica et Biophysica Acta (BBA) - General Subjects 1426(2): 239-257.

13. Burda, P. and M. Aebi (1998). "The ALG10 locus of Saccharomyces cerevisiae encodes the alpha-1,2 glucosyltransferase of the endoplasmic reticulum: the terminal glucose of the lipid-linked oligosaccharide is required for efficient N-linked glycosylation." Glycobiology 8(5): 455-462.

14. Gemmill, T. R. and R. B. Trimble (1999). "Overview of N- and O-linked oligosaccharide structures found in various yeast species." Biochimica et Biophysica Acta (BBA) - General Subjects 1426(2): 227-237.

15. Jones, J., S. S. Krag, et al. (2005). "Controlling N-linked glycan site occupancy." Biochimica et Biophysica Acta (BBA) - General Subjects 1726(2): 121-137.

16. Mitra, N., S. Sinha, et al. (2006). "N-linked oligosaccharides as outfitters for glycoprotein folding, form and function." Trends in Biochemical Sciences 31(3): 156-163.

17. Leloir, L.F. (1971). "Two decades of research on the biosynthesis of saccharides." Science. 172: 1299-1302.

18. Grunewald, W., et. al (2002). "Congenital disorders of glycosylation: a review." Pediatr. Res. 52(5): 618-624.

19. Kukuruzinska, M. A. and K. Lennon-Hopkins (1999). "ALG gene expression and cell cycle progression." Biochimica et Biophysica Acta (BBA) - General Subjects 1426(2): 359-372.

20. Kelleher, D. J., D. Karaoglu, et al. (2003). "Oligosaccharyltransferase Isoforms that Contain Different Catalytic STT3 Subunits Have Distinct Enzymatic Properties." Molecular Cell 12(1): 101-111.

21. Zhefu, M., et al. "Suppression of Insulin Receptor Substrate 1 (IRS-1) promotes mammary tumor metastasis." Mol. Cell. Biol. 26(24): 9338-9351.

22. Brogiolo, W., H. Stocker, et al. (2001). "An evolutionarily conserved function of the Drosophila insulin receptor and insulin-like peptides in growth control." Current Biology 11(4): 213-221.

23. Dickson, B.J. (2003). "Wiring the brain with insulin." Science 300: 440-441.

24. Daughaday, W. H., B. Trivedi, et al. (1993). "Serum "Big Insulin-Like Growth Factor II." from Patients with Tumor Hypoglycemia Lacks Normal E-Domain O-Linked Glycosylation, a Possible Determinant of Normal Propeptide Processing." PNAS 90(12): 5823-5827.

25. Rondinone, C. M. and D. Kramer (2002). "Proteasome inhibitors regulate tyrosine phosphorylation of IRS-1 and insulin signaling in adipocytes." Biochemical and Biophysical Research Communications 296(5): 1257-1263.

26. Shingleton, A. W., J. Das, et al. (2005). "The Temporal Requirements for Insulin Signaling During Development in Drosophila." PLoS Biology 3(9): e289.

27. Goberdhan, D. C. I. and C. Wilson (2003). "The functions of insulin signaling: size isn't everything, even in Drosophila." Differentiation 71(7): 375-397.

28. Verdu, J., M. A. Buratovich, et al. (1999). "Cell-autonomous regulation of cell and organ growth in Drosophila by Akt/PKB." Nat Cell Biol 1(8): 500-506.

29. Cho, K. S., J. H. Lee, et al. (2001). "Drosophila phosphoinositide-dependent kinase-1 regulates apoptosis and growth via the phosphoinositide 3-kinase-dependent signaling pathway." PNAS 98(11): 6144-6149.

30. Ready, D.F. (1993). Pattern formation in the *Drosophila* retina, in the development of *Drosophila melanogaster*. Cold Spring Harbor, Plainview, New York, Cold Spring Harbor Laboratory Press.

31. Dickson, B. J. (2003). "DEVELOPMENT: Wiring the Brain with Insulin." Science 300(5618): 440-441.

32. Ikeya, T., M. Galic, et al. (2002). "Nutrient-Dependent Expression of Insulin-like Peptides from Neuroendocrine Cells in the CNS Contributes to Growth Regulation in Drosophila." Current Biology 12(15): 1293-1300.

33. Junger, M., F. Rintelen, et al. (2003). "The Drosophila Forkhead transcription factor FOXO mediates the reduction in cell number associated with reduced insulin signaling." Journal of Biology 2(3): 20.

34. Puig, O. and R. Tjian (2005). "Transcriptional feedback control of insulin receptor by dFOXO/FOXO1." Genes Dev. 19(20): 2435-2446.

35. Reed, B. C., G. V. Ronnett, et al. (1981). "Role of Glycosylation and Protein Synthesis in Insulin Receptor Metabolism by 3T3-L1 Mouse Adipocytes." PNAS 78(5): 2908-2912.

36. Lee, Y.S. and Carthew, R.W. (2003). "Making a better RNAi vector for *Drosophila*: use of intron spacers." Methods 30: 322-329.

37. Gao, X., T. P. Neufeld, et al. (2000). "Drosophila PTEN Regulates Cell Growth and Proliferation through PI3K-Dependent and -Independent Pathways." Developmental Biology 221(2): 404-418.

38. Weinkove, D., T. P. Neufeld, et al. (1999). "Regulation of imaginal disc cell size, cell number and organ size by Drosophila class IA phosphoinositide 3-kinase and its adaptor." Current Biology 9(18): 1019-1029.

39. Zecca, M. and G. Struhl (2002). "Control of growth and patterning of the Drosophila wing imaginal disc by EGFR-mediated signaling." Development 129(6): 1369-1376.

40. Rome, S., K. Clement, et al. (2003). "Microarray Profiling of Human Skeletal Muscle Reveals That Insulin Regulates ~800 Genes during a Hyperinsulinemic Clamp." J. Biol. Chem. 278(20): 18063-18068.

41. Rui, L. et al. (2002). "SOCS-1 and SOCS-3 block insulin signaling by ubiquitin-mediated degradation of IRS1 and IRS2." J. Biol. Chem. 277: 42394-42398.

42. Giorgino, F., O. de Robertis, et al. (2000). "The sentrin-conjugating enzyme mUbc9 interacts with GLUT4 and GLUT1 glucose transporters and regulates transporter levels in skeletal muscle cells." PNAS 97(3): 1125-1130.

43. Frankfort, B.J. and Mardon, G. (2004) "Senseless represses nuclear transduction of Egfr pathway activation." Development 131(3): 563-70.

44. Frankfort, B.J. and Mardon, G. (2002) "R8 development in the *Drosophila* eye: a paradigm for neural selection and differentiation." Development 129: 1295-1306.

45. Hall, D.J., et. Al. (2007) "Rheb-TOR signaling promotes protein synthesis, but not glucose or amino acid import, in *Drosophila*." BMC Biology 5:10.

46. Velkey, M. (2007) "Medical Histology Learning Resources." From http://www.med.umich.edu/histology/cellsTissue/nervous.html.

Appendix

alg10 as a master regulator of N-glycosylation in STT3A-containing tissues

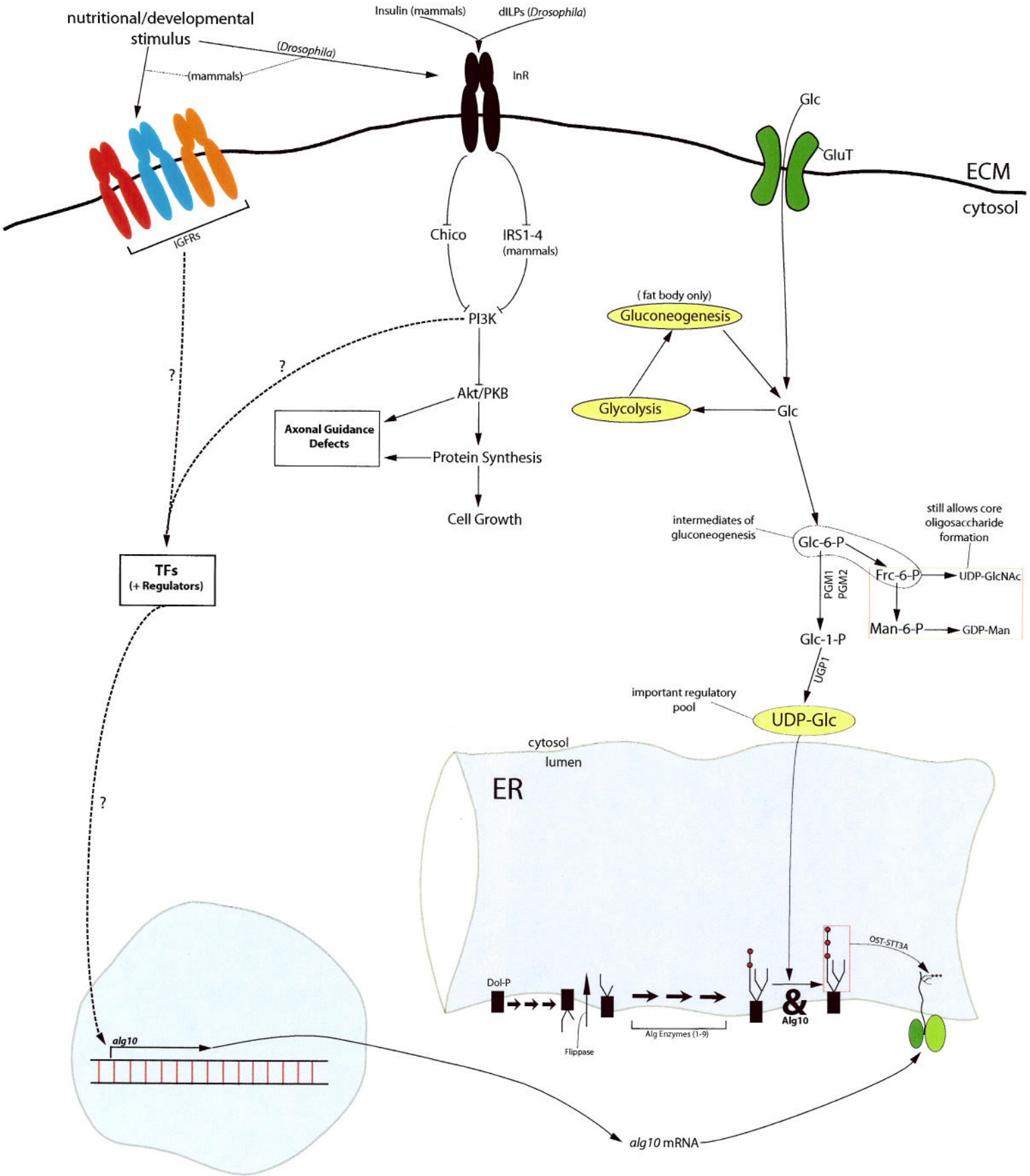

OST-STT3A-Expressing Tissue